Senescence as a main mechanism of Ritonavir and Ritonavir-NO action against melanoma

Authors: Svetlana Paskaš[1], Tamara Krajnović[1], Maria Sofia Basile[1,2], Duško Dunđerović[3], Eugenio Cavalli[4], Ferdinando Nicoletti[2], Sanja Mijatović[1], Danijela Maksimović-Ivanić[1]

Affiliations: [1]Department of Immunology, Institute for Biological Research "Siniša Stanković", Belgrade University, Belgrade, Serbia, [2]Department of Biomedical and Biotechnological Sciences, University of Catania, Catania, Italy, [3]Institute of Pathology, School of Medicine, University of Belgrade, Belgrade, Serbia, [4]IRCCS Centro Neurolesi Bonino Pulejo, Messina, Italy.

Corresponding Author: Ferdinando Nicoletti; E-mail address: ferdinic@unict.it; Postal address: Via S. Sofia 89, 95123 Catania, Italy; Phone: +390954781270.

Funding: This work was supported by the Ministry of Education, Science and Technological Development of the Republic of Serbia [grant numbers 173013 and 41031] and by the current research funds 2016 of IRCCS “Centro Neurolesi Bonino Pulejo”, Messina, Italy.

Key Words: HIV-protease inhibitors; Ritonavir; senescence; melanoma;

Abstract

The main focus of this study is exploring the effect and mechanism of two HIV-protease inhibitors (HIV-PIs): Ritonavir and Ritonavir-NO on *in vitro* growth of melanoma cell lines. Nitric oxide modification significantly improved the antitumor potential of Ritonavir, as the IC_{50} values of Ritonavir-NO were approximately two times lower than IC_{50} values of the parental compound. Our results showed for the first time, that both compounds induced senescence in primary and metastatic melanoma cell lines. This transformation was manifested as a change in cell morphology, enlargement of nuclei, increased cellular granulation, upregulation of β-galactosidase activity, lipofuscin granules appearance, higher production of ROS and persistent inhibition of proliferation. The expression of p53, as one of the key regulators of senescence, was upregulated after 48 h of Ritonavir-NO treatment only in metastatic B16F10 cells, ranking it as a late-response event. The development of senescent phenotype was consistent with the alteration of the cytoskeleton- as we observed diminished expression of vinculin, α-actin and β-tubulin. Permanent inhibition of S6 protein by Ritonavir-NO, but not Ritonavir, could be responsible for a stronger antiproliferative potential of the NO-modified compound. Taken together, induction of senescent phenotype may provide an excellent platform for developing therapeutic approaches based on selective killing of senescent cells.

1. Introduction

Melanoma incidence is rising over the past 20 years (SEER Cancer Stats Facts 2018, NIH, https://seer.cancer.gov/statfacts/html/melan.html).Therapeutic choices for melanomas are limited, and most treatments fail to improve the life quality of survived patients. Targeted therapies using MAP kinase pathway inhibitors, as well as immunotherapy using checkpoint inhibitors (CTLA4- blocking antibody, PD-1 blocking antibody), show promising results in improving the survival rates[1]. Nevertheless, the search for the most effective and tolerable drug or combination of drugs remains.

HIV-protease inhibitors (HIV-PIs) are a class of anti-retroviral drugs initially designed to target viral protease, by mimicking the viral gag-pro polyprotein and thereby blocking the active site of HIV aspartyl proteases. This action prevents production of infectious viral particles[2]. Use of HIV-PIs has coincided with a substantial reduction of incidence of HIV-associated malignant diseases including KS and some non-Hodgkin lymphoma[3,4]. Although HIV-PIs are not expected to cross-react with human proteases, preclinical data indicate that their anticancer effect may be attributed to inhibition of endopeptidases such as metalloproteinases and proteasomes[5,6]. Recent evidence demonstrate different anticancer effects of HIV-PIs both *in vitro* and *in vivo*, which are mediated through mechanisms that include: induction of apoptotic cell death, inhibition of angiogenesis, modulation of proteasome and cell cycle arrest [7-9]. Numerous mammalian proteins are affected directly by HIV-PIs, or as a consequence of their action. As a result, various toxic events that often follow long-term treatment occur, such as gastrointestinal and hepatic adverse effects, nausea, vomiting, abdominal pain and diarrhoea[10]. Other common side effects include metabolic syndrome such as dyslipidemia, insulin resistance and lipodystrophy[11]. Different modifications of HIV-PIs are explored in order to reduce the side effects and to increase the potency of these drugs. One of the approaches used for that purposes is the attachment of nitric oxide (NO) moiety. Nitric oxide decreased drug toxicity in the gastrointestinal tract by mimicking the protective role of prostaglandins and therefore,

keeping the mucosa from damage[12]. Apart from this, the most important feature of NO is its ability to inhibit cytochrome P450 or stimulate expression of P-gp[13,14]. Usually, like in the case of NSAID, NO hybridization leads to the formation of NO donating drugs. However, we have shown that the modification of HIV-PI Saquinavir exhibited a different effect[15]. Saquinavir-NO had improved anticancer potential and lower toxicity than the parental compound, without significant NO release. On different tumor cell lines Saquinavir-NO showed authentic mechanism of action through an inhibition of proliferation and induction of differentiation or transdifferentiation[16-19]. Moreover, NO-modified Saquinavir sensitized tumor cells to the natural antitumor immune response and chemotherapy[20,21]. It is known that the efficacy of Saquinavir is amplified in a combination with low doses of Ritonavir, through the ability of the later drug to inhibit cytochrome P450. Also, Ritonavir is a potent blocker, but not a substrate of ABC transporters, like other members of HIV-PIs family[22,23]. This feature, together with the potential to inhibit cytochrome P450, enables combining Ritonavir with the other drugs[24]. Accordingly, Ritonavir can be used as a booster for intestinal absorption of other HIV-PIs[25] and in liver it decreases the drug decomposition. Ritonavir was also combined with chemotherapeutic drugs like docetaxel, but also with proteasome or histone deacetylase inhibitors[26-30]. However, several data also indicated its individual antitumor action. Ritonavir was efficient on different types of solid and haematological malignancies, primarily via the induction of apoptotic cell death. It was found that Ritonavir induced caspase-dependent apoptosis and suppressed NF-κB activity in primary effusion lymphoma, a type of a non-Hodgkin lymphoma[31]. In lung adenocarcinoma it induced G0/G1 arrest and apoptosis, by down-regulating cyclin-dependent kinases, cyclin D1, and retinoblastoma protein phosphorylation[32]. G1 arrest in response to treatment was also noted in cultures of ovarian, breast, lymphoblastoid B cells, human multiple myeloma cell lines etc.[33-36]. Moreover, Ritonavir treatment led to mitochondrial damage and ROS generation in SH-SY5Y neuronal cell line[37]. In addition, Ritonavir efficacy was further confirmed in several *in vivo* models. This drug blocked the growth of lymphoma and leukemia in immunodeficient mice[34,38].

Similarly, Ritonavir inhibited breast cancer xenograft development[35]. On the basis of this background and in agreement with the enhanced anticancer action we observed by NO-hybridization of Saquinavir, we have decided to generate a NO-hybridized Ritonavir. In this study we evaluate the effects of the newly generated Ritonavir-NO in a head-to-head comparison with Ritonavir on *in vitro* growth of melanoma cell lines of different maturation status and different aggressiveness. Our results showed for the first time, that both compounds, and especially Ritonavir-NO induced senescence in primary and metastatic melanoma cell lines. Senescent cells are characterized as metabolically active, but they have lost the ability to proliferate[39]. This state of stabile growth arrest, can occur as a response to various stimuli, such as telomere shortening, activation of oncogenes, or treatment with chemotherapeutic drugs[40-42]. Since senescent cells remain viable and have the ability to secrete multitude of proteins with wide spectrum of diverse physiological functions, their existence in tumor mass can have ambivalent outcome-from tumor regression to promotion. Production of cytokines, so called senescence-associated secretory phenotype (SASP) can reinforce senescence, stimulate the clearance of senescent cells by the immune system, but also, dangerously, stimulate the growth of nearby cells[43-45]. Parallel with establishment of proliferative inability, the development of senescence is often accompanied by terminal differentiation. Melanoma is a type of tumour prone to differentiate upon treatment with diverse naturally occurring, synthetic compounds, as well as with NO-modified HIV-PI Saquinavir[16,46,47]. Beside expected differentiation toward primary melanocytes, melanoma cells can obtain Schwann-like phenotype in the process called transdifferentation[46]. All things considered, the induction of senescence and favouring its antitumor course, can be a good platform for designing new therapeutic approaches.

2. Materials and Methods

2.1. Reagents and cells

Fetal calf serum (FCS), RPMI-1640 medium, phosphate buffer saline (PBS) , dimethyl sulfoxide (DMSO), carboxy-PTIO, chloroquine diphosphate, N-acetyl-L cystein were from Sigma (St Louis, MO, USA). 5-amino-3-(4-morpholinyl)-1,2,3-oxadiazolium chloride (SIN) and N-(acetyoxy)-3-nitrosothiovaline (SNAP) were from Cayman chemical (Ann Arbor, MI, USA). Lopinavir, Lopinavir-NO, Ritonavir and Ritonavir- NO were purchased from Onconox. B16, B16F10 and A375 cell lines were purchased from American Type Culture Collection (Rockville, MD, USA). Cells were routinely maintained in HEPES-buffered RPMI-1640 medium supplemented with 10% FCS with 2 mM L-glutamine, 0.01% sodium pyruvate, 100 U/ml penicillin 100 µg/ml streptomycin, at 37°C in a humidified atmosphere with 5% CO_2.

2.2. Determination of cell viability by crystal violet and MTT assays

3000 cells/well were seeded over night and treated with tested compounds for 48 hours. After fixation and staining with 1% crystal violet (Mol, Belgrade, Serbia) for 15 min at RT, cells were washed and dried. Cells were incubated with acetic acid to dissolve crystal violet. Absorbance was measured at 540 nm. Mitochondrial dehydrogenase activity was determined by reduction of MTT (3-(4,5-dimethylthiazol-2-yl)-2,5-diphenyltetrazolium bromide). In MTT assay, cells were incubated with 0.5 mg/mL MTT (Sigma, St Louis, MO, USA) at 37°C. Incubation ended with the change of colour from yellow MTT to brown formazan, which was dissolved in DMSO. Absorbance was measured at 540 nm. In both assays, cell viability was calculated as a percentage of control (untreated cells) that was arbitrarily set to 100%.

2.3. Annexin V/ Propidium iodide staining

Melanoma cells were incubated with mixture of 1 mg/mL Annexin V-FITC (BD Pharmingen, San Diego, CA, USA) and 1 mg/mL PI (Sigma, St Louis, MO, USA) for 15 minutes at RT in the dark, diluted by adding annexin binding buffer and analyzed by flow cytometry.

2.4. Activation of caspases

Cells were trypsinized, resuspended and incubated with pan-caspase inhibitor Apostat (R&D Systems, Minneapolis, MN, USA) for 30 minutes at 37°C, washed with PBS, resuspended, and analyzed by flow cytometry.

2.5. Detection of cell proliferation

CFSE (carboxyfluorescein diacetate succinimidyl ester, Sigma, St Louis, MO, USA) was added to cells to a final concentration of 1 μM, incubated for 20 minutes at 37°C prior to treatment with HIV-protease inhibitors. Proliferation was analyzed by flow cytometry.

2.6. Measurement of ROS/RNS generation

Prior to treatment cells were incubated with DHR (Dihydrorhodamine 123, Thermo Fisher Scientific, Waltham, MA, USA) for 20 minutes at 37°C and seeded on the plate. After treatment cells were washed with PBS, trypsinized and analyzed by flow cytometry.

2.7. Measurement of intracellular nitric oxide

Intracellular NO levels were measured by staining with 2 μM DAF-FM (4-Amino-5-methylamino-2',7'-difluorofluorescein diacetate, Molecular probes, Eugen, OR, USA) for one hour at 37°C in phenol red free RPMI-1640 medium. The intensity of fluorescence was measures either by flow cytometry or a microplate reader.

2.8. Detection of autophagy

Staining with acridine orange (Lab Modena, Paris, France) in a concentration of 1 μg/ml was performed for 15 minutes at 37°C. The cells were washed, resuspended in PBS and analyzed by flow cytometry measuring green and red fluorescence.

2.9. Tyrosinase activity and melanin production

The rate of L-DOPA (3,4-dihydroxy-L-phenylalanine) (Sigma, St Louis, MO, USA) oxidation was used as an indicator of tyrosinase activity. In each sample, 1.5 million cells were incubated with 2 mg/ml L-DOPA for 15 min at 37°C. Supernatants were transferred into microtiter plates and the absorbance at 570 nm was measured. The cells were treated for 48 hours, then

trypsinized, counted and adjusted to 1.5 million/sample. Sodium hydroxide was added to lyse the cells and incubated for one hour at 60°C. The absorbance at 492 nm was measured.

2.10. Immunocytochemical detection

Cells were cultivated on glass chamber slides, treated with HIV-protease inhibitors and the expression of Myelin basic protein was detected by MBP specific antibody (#808401, Biolegend, San Diego, CA, USA). Biotinylated secondary antibody was added, followed by an incubated with extravidin peroxidase (Extravidin peroxidase staining kit, Sigma, St Louis, MO, USA) for 30 minutes. As a substrate, diaminobenzidine (Liquid plus substrate chromogen system, Agilent, Santa Clara, CA, USA) was used. Counterstaining was done with Mayer's haematoxylin (Sigma, St Louis, MO, USA) and the slides were mounted with glycerine gel (Agilent, Santa Clara, CA, USA).

2.11. Clonogenic assay

Colony forming assay was used to determine the cytostatic effect of HIV-PIs. Melanoma cells were treated for 48h with Ritonavir and Ritonavir-NO, trypsinized and seeded in a concentration 1000 cells/ well. The formation of colonies was followed for 7 days. After that, cells were fixated, stained with crystal violet and counted using Image J program (version 1.50i, NIH, Bethesda, MD, USA). The fraction of cells that retained the capacity to produce colonies was calculated by dividing plating efficiency of treated cells with plating efficiency of control.

2.12. β-galactosidase assay

Melanoma cells were stained with β-galactosidase substrate FDG (Fluorescein digalactoside, Molecular probes, Eugene, OR, USA) to a final concentration of 1mM. After 1 min incubation at 37^{o}C, cells were analyzed by flow cytometry.

2.13. Western blot

Cell lysates (20 μg) were separated by 12% SDS-PAGE, electro blotted onto PVDF membrane (Merck, Burlington, MA, USA), blocked with 5%BSA in TBS-Tween (50 mM TrisHCl pH7.6, 150 mM NaCl, 0.05% Tween 20), and probed with primary antibody over night at 4°C. After washing,

membranes were incubated with horseradish peroxidase- conjugated secondary antibody (Santa Cruz Biotechnology, Dallas,TX, USA). Immunoreactive bands were identified by ECL chemiluminiscence detection system (GE Healthcare, Buckinghamshire, UK) according to manufacturer's instructions. Following primary antibodies were used: phospho-P70S6K (Cell Signalling Technology #9205), P70S6K (Cell Signalling Technology #9202), phospho-S6 (Cell Signalling Technology #2215), S6 antibody (Cell Signalling Technology #2217), β-actin (Sigma #8254), Notch (Santa Cruz, sc-91703), Oct (Santa Cruz sc-9081), β-catenin (Santa Cruz, sc-7199), vinculin (Sigma #V9131), α-tubulin (Cell Signalling Technology #2125), GAPDH (Abcam, ab9483).

2.14. Lipofuscin staining

Cells were cultivated on glass chamber slides, treated with HIV-protease inhibitors for indicated time. At the end of the incubation period, cells were fixed, permeabilized with 3%H_2O_2 in 10 % methanol in PBS and stained with Sudan 3 dye as suggested by the manufacturer. Finally, glass slides were mounted and analyzed by Olympus BX50 microscope (Olympus, Tokyo, Japan) with Olympus DP70 camera, 1000x magnification. Slides were also used for calculation of nuclear/ cytoplasm (N/C) ratio using ImageJ.

2.15. Statistical analysis

Statistical Package for the Social Sciences (SPSS, IBM, Armonk, NY, USA) was used for data analysis. Student t-test and ANOVA (with post-hoc Tukey test) were performed as parametric tests, and Mann-Whitney and Kruskal-Wallis tests were performed as non-parametric. To examine if variables are normally distributed, the Kolmogorov Smirnov test was used.

3. Results

3.1. Ritonavir-NO affects viability of melanoma cells *in vitro* more potently than the original drug

Human melanoma A375 cells, mouse solid melanoma B16 and its metastatic clone B16F10 cells were treated with concentration range starting from 1.25 to 80 μM of Ritonavir and Ritonavir-NO for 48 h. Cell viability was estimated using crystal violet and MTT assays. As presented in Supplement S1, both compounds significantly diminished cell viability in a dose dependent manner. However, Ritonavir-NO was more effective than parental drug, having IC_{50} values approximately two times lower in all three cell lines (Table 1). Results obtained by both tests were synchronized indicated that mitochondrial respiration as well as DNA/RNA content appropriately reflected number of viable cells. Importantly, while Ritonavir activity showed tendency to decline depending on the metastatic properties of cell lines, the efficacy of its NO modified counterpart was persistent.

3.2. The antitumor activity of Ritonavir and Ritonavir- NO is based primarily on their cytostatic effect

Cells were treated with IC_{50} dose of each compound for 48 h when the analyses of cellular proliferation and cell death were performed. Staining of B16 cells with CFSE revealed inhibition of cellular proliferation upon treatment with both compounds, while the capacity of NO modified compound was more profound (Figure 1A). Nevertheless, both drugs inhibited proliferation in approximately 60% of cells in metastatic melanoma cell line, indicating that those cells have a greater sensitivity towards used HIV-PIs. Since the IC_{50} of Ritonavir-NO is more than twice lower than original, it is obvious that applied chemical intervention augmented the original anticancer potential. In parallel, double staining with Annexin V/ PI did not show significant presence of apoptotic or necrotic cells (Figure 1B). Even in the absence of apoptosis, activation of caspases was detected in B16 melanoma cell line. Having in mind that apostat marks all activated caspases, enzymes with important role in many process apart from apoptosis, the observed data suggest their involvement in processes different from cell death (Figure 1C). Nuclear staining with propidium iodide revealed majority of large euchromatic nuclei in HIV-PI treated samples. Only few segmented nuclei typical of apoptotic nuclear destruction were

observed in same samples (Figure 1D) confirming previously stated minor apoptosis accompanied with cell division blockade. Further on, we followed the development of acridine orange positive autophagosomes as markers of autophagy by flow cytometry. The intensity of fluorescence slightly increased upon treatment with Ritonavir and Ritonavir-NO in B16 cell line: 5.6% and 5.7% and in B16F10: 2.6% and 0.6% for Ritonavir and Ritonavir-NO, respectively (data not shown), excluding autophagy as an effect of tested drugs. In summary, apoptosis is just a minor effect, indicating that inhibition of proliferation is mainly responsible for decreased cell viability.

3.3. Tested HIV-PIs do not direct differentiation of melanoma cells toward melanocytes nor Schwann-like cells

In vitro treatment with both Ritonavir and Ritonavir-NO was accompanied by morphological transformation of B16 and B16F10 cells. This effect was observed with light microscopy, accompanied by morphologic transformation, suggesting a possible differentiation process (Supplement S2). Namely, the cells obtained flatten rhomboid shape with elongated dendritic like extensions.

Additionally, B16 and B16F10 cells treated with Ritonavir and Ritonavir-NO showed remarkable enhanced cell size (2.87; 5.4; 7.5 and 2.54; 5.7; 7.7, measured as pixels in control, Ritonavir and Ritonavir-NO, in B16 and B16F10, respectively). Calculation of nuclear/cytoplasmic ratio (N/C), by ImageJ analysis, confirmed that treated cells lost their malignant properties. While in control B16 cells N/C ratio was 0.54, it declined to 0.2 and 0.23 upon the exposure to Ritonavir and Ritonavir-NO. This effect was even more pronounced in metastatic clone (N/C ratio was 0.58; 0.24; 0.17 in control, Ritonavir and Ritonavir-NO, respectively).

In order to determine the course of differentiation, three basic functional tests were preformed: measurement of melanin levels, the tyrosinase activity and expression of MBP (Schwann-like cell marker). As shown in Figure 2A, melanin levels and tyrosinase activity were unaltered in treated vs. control cells. Surprisingly, HIV-PI treatment did not lead to a significant elevation of

MBP expression in B16 and B16F10 cells (Figure 2B), suggesting that cells didn't acquire melanocytic or Schwann like phenotype. Observed change in cell morphology is typical for senescent phenotype even in the absence of the markers of terminal differentiation. In concordance, flow cytometric analysis discovered an increase in SSC, a parameter of cell granularity, confirming that cells upon the treatment with HIV-PIs entered the senescent state (Supplement S3). Previously noticed difference in Ritonavir/Ritonavir-NO behaviour in primary vs. metastatic cell line was reflected in the aspect of cellular granularity. While in B16 cell line Ritonavir-NO triggered more intensive granularity in comparison to maternal drug, in invasive counterpart both drugs were capable to introduce cells in senescent phenotype.

3.4. Senescence is the main mechanism of Ritonavir and Ritonavir-NO action

β-galactosidase activity is a gold standard for evaluation of cellular senescence. In presented experimental setting, the activity of β-galactosidase significantly increased in HIV-PI treated primary and metastatic melanoma (Figure 3A), indicating that a mode of action of tested drugs was initiated by differentiation, and guided toward senescent phenotype with reduced proliferation capacity. It has been demonstrated that lipofuscin aggregates, formed from oxidised proteins, co-localized with β-galactosidase in senescent cells[48]. The treatment with both compounds elevated the presence of lipofuscin granules in both B16 and B16F10 cells, confirming once more the induction of senescence as a response to HIV-protease inhibitors treatment (Figure 3B). Having in mind that senescent phenotype might be a transitory state, influenced by the drugs presence. Further on, we investigated the persistence of this effect on melanoma cells by performing a clonogenic assay. A decrease in a number and size of colonies in comparison to untreated B16 cells was detected after exposure to both HIV-PIs. On the other hand, we noticed a reduction in the colony surface only in metastatic clone (Figure 3C). Both findings strongly suggest that loss of dividing potential, as a consequence of treatment, was stable even in the absence of drugs. Having in mind that p53 is a central player in senescence establishment, and that this process is followed by the alteration of the cytoskeleton, the

influence of HIV-PIs on their expression was evaluated. While the expression of vinculin, α-tubulin and β-actin was down-regulated by both NO-modified and the original drug, the expression of p53 stabilized form (phosphorylation of Ser 20) was significantly enhanced in invasive F10 clone of B16 cells only upon Ritonavir-NO treatment (Supplement 4). Taken together, development of senescence in response to the treatment was not dependent on the type of HIV-PIs or the maturity of B16 cells.

3.5. Ritonavir-NO does not release nitric oxide

Intracellular NO was detected by the DAF-FM diacetate. Our data suggest that Ritonavir-NO, as a potential donor, did not release nitric oxide (Figure 4A). Further on, we investigated the possible generation of reactive oxygen and nitrogen species in Ritonavir-NO treated cells, by measuring intracellular DHR123 fluorescence. The intracellular production of ROS/RNS was markedly elevated for both HIV-PIs in primary and metastatic melanoma (Figure 4B). Neutralization by the antioxidant N-acetylcystein did not improve the viability of treated cells, indicating that production of ROS is an additional manifestation of senescence (Supplement S5).

3.6. Ritonavir and Ritonavir-NO intracellular signalling

Finally, we investigated signalling pathways involved in a cellular decision to self-renew or to differentiate, by following the expression of Notch-1, Oct3/4 transcription factor, β-catenin, p70S6 kinase and S6 protein. Notch-1 expression was transiently downregulated in B16 cell line, while in B16F10, in cells treated with Ritonavir-NO there is a temporary upregulation, suggesting that only NO-modified compound is equally potent to inhibit Notch-1 in primary and metastatic melanoma (Figure 5). The expression of Oct3/4 after 48h was down regulated upon treatment with both compounds, but with a more profound effect in an invasive F10 subclone (Figure 5). The expression of β-catenin was less affected by NO-modified drug in both cell lines. Namely, a strong decline in β-catenin expression observed in B16 cells was weakened by NO addition to the drug. In parallel, in B16F10 cells, the potential of Ritonavir to inhibit β-catenin

after chemical intervention was converted into its potentiation (Figure 5). This could be ascribed to progenitor features of invasive subclone. On the other hand, Ritonavir induced permanent inhibition of p70S6K in both cell lines (Figure 6). This inhibition was not accompanied with inhibited expression of S6 protein. Moreover of transient but strong upregulation of S6 protein was observed. Oppositely, NO-modified drug showed diverse effect on p70S6K expression in two melanoma cell lines. In B16 cells, upregulation of this protein was detected after the treatment, while in low differentiated counterpart its expression was suppressed (Figure 6). Phosphorylation of downstream target of p70S6K, S6 protein was decreased in both cell lines upon the treatment with Ritonavir-NO. Having in mind that this protein is directly responsible for proliferative response of cells to different mitogenic stimuli[49], its permanent inhibition by Ritonavir-NO but not Ritonavir can explain stronger antiproliferative potential of newly designed compound.

4. Discussion

Strategies for antitumor therapy are constantly changing and improving. A big breakthrough was initiated when apoptosis was used as novel anticancer approach. However, the discovery of apoptosis-induced proliferation, which results in tumor repopulation, made way for a better characterization of compensatory mechanisms[50,51]. During the last 10 years, a pro-senescent therapy, or senescence-inducing therapy has emerged as another tumor deifying strategy[40,41]. Once the cells obtain the senescent phenotype, they remain viable and metabolically active but with permanent growth arrest[39]. Blockage at the G1 or G2/M phases of the cell cycle hinders cells to proceed with division even after mitogen stimulation. It is known that senescencent melanocytes in human skin nevi, remain indolent for years[52]. Nevertheless, senescent cells can be cleared *in vivo* by an immune system[45,53].

Here we present a novel mechanism of two HIV-protease inhibitors, Ritonavir and its NO-derivative. These compounds induce development of a senescent phenotype. HIV-protease

inhibitors are established as antitumor agents with broad spectrum of mechanisms in different cancer types[54]. NO-modification significantly improved antitumor potential of Ritonavir. Viability assays clearly evidence that IC_{50} values of Ritonavir-NO are approximately two times lower than IC_{50} values of parental compound. These results are concordant to previous studies on NO-modified Saquinavir and Lopinavir[16,19,55]. Covalently attaching NO to mentioned HIV-PIs increased the efficacy and reduced the toxicity of the compounds. Interestingly, the efficacy of Ritonavir-NO is stable independently of the invasive and metastatic properties of tested cell lines, thus presenting the advantage of modified drug to original one and underlining again that NO attachment to HIV-PIs is a useful approach for improvement of this class of compounds.

One of the main modes of HIV-PIs action is the induction of cell death, mediated by caspase activity. In this study, we have detected an increase in the activation of caspases only in less aggressive melanoma cell line, indicating a different mechanism in high- and low-differentiated melanomas. Activation of caspases was not followed by apoptosis, namely, apoptosis was a minor effect in both cell lines. Different to Ritonavir and Ritonavir-NO, Saquinavir and its NO derivate induced a strong apoptosis in PC-3 cells and leukaemia cells[18,55]. These data reveal that protease inhibitors do not provoke a single type of response in cancer cells, but a whole range of different mechanisms are activated, depending on the cancer type, differentiation status and metastatic potential.

Inhibition of proliferation is another hallmark of anticancer action of HIV-PIs. This study confirms that Ritonavir and Ritonavir-NO exhibit a stronger antiproliferative potential in metastatic melanoma. Previous studies postulate a significant potential for proliferation inhibition of Saquinavir[16,17]. Inhibition of proliferation can be accompanied by a cell differentiation, since these two processes are inversely regulated[56]. Therefore, we investigated the effect of tested compounds on melanoma cell differentiation. Melanoma can differentiate further to melanocytes or to a glial phenotype, characterized by a loss of melanogenesis, a change in cell morphology and the expression of early Schwann cell markers, such as myelin basic protein (MBP) and

protein zero (P0) [57-61]. In this study, testing for differentiation into melanocytes and Schwann-like cells was negative, and in addition, according to the expression of □-galactosidase and lipofuscin granules[48,62], we observed senescent cells after 48h treatment with Ritonavir and Ritonavir-NO. It was previously found that Ritonavir in a combination with Lopinavir induces osteoblast senescence and alter adypocyte differentiation in bone marrow MSCs[63]. Cultured *in vitro*, senescent cells develop a distinct and recognizable flattened and enlarged morphology with a prominent nucleus and increased cytoplasmic granularity[42,64,65]. The senescent morphology was confirmed by a flow cytometry as an increase in side scatter parameter. Recent findings link autophagy to cellular senescence. During the cell transition from mitotic to senescent, an extensive cell remodelling occurs, which consequently activates autophagy[66]. In our study, autophagy was detected at a very low level, excluding its contribution to senescence. Goehe et al. reported that in breast and colon carcinoma cells senescence was independent of autophagy and occurred even when autophagy was suppressed[67]. The most important fact, for unravelling the basic mechanism of Ritonavir and Ritonavir-NO triggered senescence is the ability of these drugs to inhibit proteasome activity in mammalian cells[9,68]. Namely, oxidized and cross-linked protein aggregates such as lipofuscin, age pigments etc. that are key markers of aging and senescence, accumulated due to disturbed proteosomal degradation[69].

Production of reactive oxygen species is another characteristic of senescent cells, and we investigated the possible generation of ROS/RNS in Ritonavir and Ritonavir-NO treated cells, by using intracellular fluorophore DHR 123. Indeed, the production of ROS/RNS was increased, indicating that reactive oxygen and nitrogen species could play a role in the induction and maintenance of cell senescence, as shown in previous studies[70,71]. Incubation of B16 cells with an antioxidant N-acetylcistein validated that oxidative stress is not responsible for a decrease of cell viability, and that it is probably a manifestation of senescence. Moreover, we detect just slight intracellular nitric oxide in response to both treatments indicating that Ritonavir-NO didn't

function as NO donating drug. In the family of NO-modified HIV-PIs, Saquinavir-NO showed similar feature, suggesting that chemical intervention generated qualitatively new drug[16,17]. Clonogenic assay provides the proof of the irreversible proliferation arrest after a period of compound-free growth post-treatment. Saquinavir reduced clonogenicity of HeLa cells after 96h of treatment[68]. In this study, clonogenic effect was observed after 48 h of treatment, and 5 days of cell cultivation without Ritonavir and Ritonavir-NO, evidencing a long-lasting effect of these compounds on colony formation.

The expression of p53, as one of the key regulators of senescence, was upregulated after 48 h of Ritonavir-NO treatment only in metastatic B16F10 cells, ranking it as a late-response event. Phosphorylation of Ser20 is important for stabilization of p53 and enhancement of its transcriptional activity[72]. Xue et al. reported that p53 activation in murine liver carcinoma induced cellular senescence program, and that p53 loss is a characteristic of aggressive carcinomas[73]. B16 and B16F10 cell lines used in this study have p53 wt status[74] despite the differentiation status. However, recently it was demonstrated that cellular senescence is possible even without p53 involvement. The development of senescent phenotype was supported by the alteration of cellular skeleton. Independent of the drug type or the cell line used, we observed diminished vinculin, α-actin and β-tubulin expression. Similarly, the development of senescence in human fibroblasts correlated with down regulation of actin and tubulin expression[76]. On the other hand, it has been reported that the expression, but not the distribution of vinculin, was not changed in senescent fibroblasts in response to the hydrogen peroxide[77]. In detail, edge accumulated form of vinculin was replaced with randomly and sporadically expressed throughout senescent phenotype. Decreased vinculin presence determined in this study can be connected to abrogated malignancy of melanoma cells since it was found that vinculin regulates mechanical properties like: contractility, adhesion strength, stiffness and the ability of cells to invade and metastasize[78]. The analysis of Notch-1, Oct3/4 and β-catenin expression revealed that in B16 cells treatment both compounds negatively

regulated all tested proteins. Having in mind that intensified Notch-1 expression is found in early neoplastic lesions and it is considered to be important for tumor progression[79], inhibited expression of this protein by HIV-PIs, can be a valuable effect. Interestingly, the expression pattern of analysed proteins in invasive form of melanoma was quite different. While Notch-1 was transiently down regulated, inhibition of Oct3/4 was persistent and time dependent. However, β-catenin was not affected by the treatment with modified drug. Moreover, the dynamic of change of its expression was inversely regulated in comparison to Notch-1. It was recently published that in progenitor cells, such as low differentiated B16F10, β-catenin protein is negatively regulated by Notch[80]. Potentiated amount of β-catenin in Ritonavir-NO treated cells can explain its strong antiproliferative potential since it was found that β-catenin is responsible for G2M arrest in normal as well as in transformed cells[81]. Strong, persistent inhibition of Oct3/4 in invasive subclone of F10 can be responsible for vinculin abolishment, since it was found that this protein regulates vinculin expression in highly aggressive cancer of neuroectodermal origin[82]. Finally, while p70S6K activity was strongly suppressed by both compounds in invasive clone, its expression in less aggressive cell line was even potentiated, indicating the relevance of the cell specificity on drugs action. Similar inhibition of p70S6K was found in haematological cell lines upon Saquinavir-NO exposure, indicating it as a potential target for NO-hybridized HIV-PIs[55]. In this study, p70S6 was oppositely regulated in low and high invasive cells, while its downstream target S6 protein was down regulated in a similar manner in both cell lines, suggesting that S6 is a direct target of the drug. It is known that S6 protein is initially included in protein synthesis and response to mitogens, therefore, obtained result could be an explanation of a strong anti-proliferative capacity of Ritonavir-NO[49]. Moreover, the rpS6 regulated actin cytoskeleton so its inhibition might be related to observed change in cellular morphology[83,84]. Finally, the inhibition of mTOR pathway is implicated in the senescence establishment upon chronic radiation[85]. Different regulation of S6 protein by Ritonavir and Ritonavir-NO, with remarkably higher potency of modified drug to down-regulate S6 expression, can be accounted

for enhanced antitumor efficacy of Ritonavir-NO, and even more, can explain why modified Ritonavir possesses a persistent ability to downregulate metastatic cell growth *in vitro* while in parallel, Ritonavir was weaker. To summarize, in the study presented here, we provide evidence for an *in vitro* senescence induced by Ritonavir and Ritonavir-NO, in a treatment of primary and metastatic melanoma cell lines. The development of senescent-like phenotype accompanied by a permanent loss of dividing potential, may provide an excellent platform for the increment of therapeutic approaches based on selective killing of senescent cells. Having in mind that Ritonavir can elevate the efficacy of numerous drugs due to the inhibition of cytochrome P450 or P-gp[86], an additional aspect of future studies is combining a treatment of novel drugs with conventional therapy. Finally, two modified HIV-PIs, Saquinavir and Lopinavir, were found to be efficient in several *in vivo* tumor models, creating a good platform for further investigation of antitumor properties of members of this class of compounds, such as Ritonavir-NO[16,17,87-89].

Conflicts of interest: F.N. is a cofounder and shareholder of OncoNOx.

5. References

1 Romano E, Michielin O. Successes and limitations of targeted cancer therapy in melanoma. *Prog Tumor Res*. 2014;41:78-88.

2 Flexner C. HIV-protease inhibitors. *N Engl J Med*. 1998;338:1281-1292.

3 Boshoff C, Weiss R. AIDS-related malignancies. *Nat Rev Cancer*. 2002;2:373-382.

4 Sgadari C, Barillari G, Toschi E *, et al.* HIV protease inhibitors are potent anti-angiogenic molecules and promote regression of Kaposi sarcoma. *Nat Med*. 2002;8:225-232.

5 Pajonk F, Himmelsbach J, Riess K *, et al.* The human immunodeficiency virus (HIV)-1 protease inhibitor saquinavir inhibits proteasome function and causes apoptosis and

radiosensitization in non-HIV-associated human cancer cells. *Cancer Res*. 2002;62:5230-5235.

6 Chow WA, Jiang C, Guan M. Anti-HIV drugs for cancer therapeutics: back to the future? *Lancet Oncol*. 2009;10:61-71.

7 Toschi E, Sgadari C, Malavasi L *, et al.* Human immunodeficiency virus protease inhibitors reduce the growth of human tumors via a proteasome-independent block of angiogenesis and matrix metalloproteinases. *Int J Cancer*. 2011;128:82-93.

8 Xiang T, Du L, Pham P *, et al.* Nelfinavir, an HIV protease inhibitor, induces apoptosis and cell cycle arrest in human cervical cancer cells via the ROS-dependent mitochondrial pathway. *Cancer Lett*. 2015;364:79-88.

9 Andre P, Groettrup M, Klenerman P *, et al.* An inhibitor of HIV-1 protease modulates proteasome activity, antigen presentation, and T cell responses. *Proc Natl Acad Sci U S A*. 1998;95:13120-13124.

10 Keeble JE, Moore PK. Pharmacology and potential therapeutic applications of nitric oxide-releasing non-steroidal anti-inflammatory and related nitric oxide-donating drugs. *Br J Pharmacol*. 2002;137:295-310.

11 Powderly WG. Long-term exposure to lifelong therapies. *J Acquir Immune Defic Syndr*. 2002;29 Suppl 1:S28-40.

12 Singh R, Kumar R, Singh DP. Nitric oxide-releasing nonsteroidal anti-inflammatory drugs: gastrointestinal-sparing potential drugs. *J Med Food*. 2009;12:208-218.

13 Minamiyama Y, Takemura S, Imaoka S *, et al.* Irreversible inhibition of cytochrome P450 by nitric oxide. *J Pharmacol Exp Ther*. 1997;283:1479-1485.

14 Dixit SG, Zingarelli B, Buckley DJ *, et al.* Nitric oxide mediates increased P-glycoprotein activity in interferon-{gamma}-stimulated human intestinal cells. *Am J Physiol Gastrointest Liver Physiol*. 2005;288:G533-540.

15 Fiorucci S, Antonelli E, Burgaud JL *, et al.* Nitric oxide-releasing NSAIDs: a review of their current status. *Drug Saf*. 2001;24:801-811.

16 Maksimovic-Ivanic D, Mijatovic S, Miljkovic D *, et al.* The antitumor properties of a nontoxic, nitric oxide-modified version of saquinavir are independent of Akt. *Mol Cancer Ther*. 2009;8:1169-1178.

17 Mojic M, Mijatovic S, Maksimovic-Ivanic D *, et al.* Therapeutic potential of nitric oxide-modified drugs in colon cancer cells. *Mol Pharmacol*. 2012;82:700-710.

18 Mojic M, Mijatovic S, Maksimovic-Ivanic D *, et al.* Saquinavir-NO-targeted S6 protein mediates sensitivity of androgen-dependent prostate cancer cells to TRAIL. *Cell Cycle*. 2012;11:1174-1182.

19 Mijatovic S, Maksimovic-Ivanic D, Mojic M *, et al.* Cytotoxic and immune-sensitizing properties of nitric oxide-modified Saquinavir in iNOS-positive human melanoma cells. *J Cell Physiol*. 2011;226:1803-1812.

20 Maksimovic-Ivanic D, Fagone P, McCubrey J *, et al.* HIV-protease inhibitors for the treatment of cancer: Repositioning HIV protease inhibitors while developing more potent NO-hybridized derivatives? *Int J Cancer*. 2017;140:1713-1726.

21 Rothweiler F, Michaelis M, Brauer P *, et al.* Anticancer effects of the nitric oxide-modified saquinavir derivative saquinavir-NO against multidrug-resistant cancer cells. *Neoplasia*. 2010;12:1023-1030.

22 Bierman WF, Scheffer GL, Schoonderwoerd A *, et al.* Protease inhibitors atazanavir, lopinavir and ritonavir are potent blockers, but poor substrates, of ABC transporters in a broad panel of ABC transporter-overexpressing cell lines. *J Antimicrob Chemother*. 2010;65:1672-1680.

23 Gupta A, Zhang Y, Unadkat JD *, et al.* HIV protease inhibitors are inhibitors but not substrates of the human breast cancer resistance protein (BCRP/ABCG2). *J Pharmacol Exp Ther*. 2004;310:334-341.

24 Rock BM, Hengel SM, Rock DA *, et al.* Characterization of ritonavir-mediated inactivation of cytochrome P450 3A4. *Mol Pharmacol*. 2014;86:665-674.

25 Holmstock N, Annaert P, Augustijns P. Boosting of HIV protease inhibitors by ritonavir in the intestine: the relative role of cytochrome P450 and P-glycoprotein inhibition based on Caco-2 monolayers versus in situ intestinal perfusion in mice. *Drug Metab Dispos*. 2012;40:1473-1477.

26 Isono M, Sato A, Asano T *, et al.* Delanzomib Interacts with Ritonavir Synergistically to Cause Endoplasmic Reticulum Stress in Renal Cancer Cells. *Anticancer Res*. 2018;38:3493-3500.

27 Hendrikx JJ, Lagas JS, Song JY *, et al.* Ritonavir inhibits intratumoral docetaxel metabolism and enhances docetaxel antitumor activity in an immunocompetent mouse breast cancer model. *Int J Cancer*. 2016;138:758-769.

28 Liu R, Zhang L, Yang J *, et al.* HIV Protease Inhibitors Sensitize Human Head and Neck Squamous Carcinoma Cells to Radiation by Activating Endoplasmic Reticulum Stress. *PLoS One*. 2015;10:e0125928.

29 Kraus M, Muller-Ide H, Ruckrich T *, et al.* Ritonavir, nelfinavir, saquinavir and lopinavir induce proteotoxic stress in acute myeloid leukemia cells and sensitize them for proteasome inhibitor treatment at low micromolar drug concentrations. *Leuk Res*. 2014;38:383-392.

30 Sato A, Asano T, Ito K. 17-Allylamino-17-demethoxygeldanamycin and ritonavir inhibit renal cancer growth by inhibiting the expression of heat shock factor-1. *Int J Oncol*. 2012;41:46-52.

31 Kariya R, Taura M, Suzu S *, et al.* HIV protease inhibitor Lopinavir induces apoptosis of primary effusion lymphoma cells via suppression of NF-kappaB pathway. *Cancer Lett*. 2014;342:52-59.

32 Srirangam A, Milani M, Mitra R *, et al.* The human immunodeficiency virus protease inhibitor ritonavir inhibits lung cancer cells, in part, by inhibition of survivin. *J Thorac Oncol*. 2011;6:661-670.

33 Kumar S, Bryant CS, Chamala S *, et al.* Ritonavir blocks AKT signaling, activates apoptosis and inhibits migration and invasion in ovarian cancer cells. *Mol Cancer*. 2009;8:26.

34 Dewan MZ, Tomita M, Katano H *, et al.* An HIV protease inhibitor, ritonavir targets the nuclear factor-kappaB and inhibits the tumor growth and infiltration of EBV-positive lymphoblastoid B cells. *Int J Cancer*. 2009;124:622-629.

35 Srirangam A, Mitra R, Wang M *, et al.* Effects of HIV protease inhibitor ritonavir on Akt-regulated cell proliferation in breast cancer. *Clin Cancer Res*. 2006;12:1883-1896.

36 Ikezoe T, Hisatake Y, Takeuchi T *, et al.* HIV-1 protease inhibitor, ritonavir: a potent inhibitor of CYP3A4, enhanced the anticancer effects of docetaxel in androgen-independent prostate cancer cells in vitro and in vivo. *Cancer Res*. 2004;64:7426-7431.

37 Tricarico PM, de Oliveira Franca RF, Pacor S *, et al.* HIV Protease Inhibitors Apoptotic Effect in SH-SY5Y Neuronal Cell Line. *Cell Physiol Biochem*. 2016;39:1463-1470.

38 Dewan MZ, Uchihara JN, Terashima K *, et al.* Efficient intervention of growth and infiltration of primary adult T-cell leukemia cells by an HIV protease inhibitor, ritonavir. *Blood*. 2006;107:716-724.

39 Campisi J, d'Adda di Fagagna F. Cellular senescence: when bad things happen to good cells. *Nat Rev Mol Cell Biol*. 2007;8:729-740.

40 Campisi J. Aging, cellular senescence, and cancer. *Annu Rev Physiol*. 2013;75:685-705.

41 Collado M, Serrano M. Senescence in tumours: evidence from mice and humans. *Nat Rev Cancer*. 2010;10:51-57.

42 Ewald JA, Desotelle JA, Wilding G *, et al.* Therapy-induced senescence in cancer. *J Natl Cancer Inst*. 2010;102:1536-1546.

43 Coppe JP, Patil CK, Rodier F *, et al.* Senescence-associated secretory phenotypes reveal cell-nonautonomous functions of oncogenic RAS and the p53 tumor suppressor. *PLoS Biol*. 2008;6:2853-2868.

44 Krtolica A, Parrinello S, Lockett S *, et al.* Senescent fibroblasts promote epithelial cell growth and tumorigenesis: a link between cancer and aging. *Proc Natl Acad Sci U S A*. 2001;98:12072-12077.

45 Hoenicke L, Zender L. Immune surveillance of senescent cells--biological significance in cancer- and non-cancer pathologies. *Carcinogenesis*. 2012;33:1123-1126.

46 Mijatovic S, Bramanti A, Nicoletti F *, et al.* Naturally occurring compounds in differentiation based therapy of cancer. *Biotechnol Adv*. 2018;

47 Bulatovic MZ, Maksimovic-Ivanic D, Bensing C *, et al.* Organotin(IV)-loaded mesoporous silica as a biocompatible strategy in cancer treatment. *Angew Chem Int Ed Engl*. 2014;53:5982-5987.

48 Salmonowicz H, Passos JF. Detecting senescence: a new method for an old pigment. *Aging Cell*. 2017;16:432-434.

49 Hutchinson JA, Shanware NP, Chang H *, et al.* Regulation of ribosomal protein S6 phosphorylation by casein kinase 1 and protein phosphatase 1. *J Biol Chem*. 2011;286:8688-8696.

50 Huang Q, Li F, Liu X *, et al.* Caspase 3-mediated stimulation of tumor cell repopulation during cancer radiotherapy. *Nat Med*. 2011;17:860-866.

51 Ryoo HD, Bergmann A. The role of apoptosis-induced proliferation for regeneration and cancer. *Cold Spring Harb Perspect Biol*. 2012;4:a008797.

52 Michaloglou C, Vredeveld LC, Soengas MS *, et al.* BRAFE600-associated senescence-like cell cycle arrest of human naevi. *Nature*. 2005;436:720-724.

53 Kang TW, Yevsa T, Woller N *, et al.* Senescence surveillance of pre-malignant hepatocytes limits liver cancer development. *Nature*. 2011;479:547-551.

54 Bernstein WB, Dennis PA. Repositioning HIV protease inhibitors as cancer therapeutics. *Curr Opin HIV AIDS*. 2008;3:666-675.

55 Maksimovic-Ivanic D, Mojic M, Bulatovic M *, et al.* The NO-modified HIV protease inhibitor as a valuable drug for hematological malignancies: Role of p70S6K. *Leuk Res*. 2015;39:1088-1095.

56 Ruijtenberg S, van den Heuvel S. Coordinating cell proliferation and differentiation: Antagonism between cell cycle regulators and cell type-specific gene expression. *Cell Cycle*. 2016;15:196-212.

57 Kamaraju AK, Bertolotto C, Chebath J *, et al.* Pax3 down-regulation and shut-off of melanogenesis in melanoma B16/F10.9 by interleukin-6 receptor signaling. *J Biol Chem*. 2002;277:15132-15141.

58 Slutsky SG, Kamaraju AK, Levy AM *, et al.* Activation of myelin genes during transdifferentiation from melanoma to glial cell phenotype. *J Biol Chem*. 2003;278:8960-8968.

59 Reed JA, Finnerty B, Albino AP. Divergent cellular differentiation pathways during the invasive stage of cutaneous malignant melanoma progression. *Am J Pathol*. 1999;155:549-555.

60 Ivanov VN, Hei TK. Regulation of viability, differentiation and death of human melanoma cells carrying neural stem cell biomarkers: a possibility for neural trans-differentiation. *Apoptosis*. 2015;20:996-1015.

61 Larribere L, Utikal J. De- and re-differentiation of the melanocytic lineage. *Eur J Cell Biol*. 2014;93:30-35.

62 Georgakopoulou EA, Tsimaratou K, Evangelou K *, et al.* Specific lipofuscin staining as a novel biomarker to detect replicative and stress-induced senescence. A method applicable in cryo-preserved and archival tissues. *Aging (Albany NY)*. 2013;5:37-50.

63 Hernandez-Vallejo SJ, Beaupere C, Larghero J *, et al.* HIV protease inhibitors induce senescence and alter osteoblastic potential of human bone marrow mesenchymal stem cells: beneficial effect of pravastatin. *Aging Cell*. 2013;12:955-965.

64 Mehta IS, Figgitt M, Clements CS *, et al.* Alterations to nuclear architecture and genome behavior in senescent cells. *Ann N Y Acad Sci*. 2007;1100:250-263.

65 Narita M. Cellular senescence and chromatin organisation. *Br J Cancer*. 2007;96:686-691.

66 Hoare M, Young AR, Narita M. Autophagy in cancer: having your cake and eating it. *Semin Cancer Biol*. 2011;21:397-404.

67 Goehe RW, Di X, Sharma K *, et al.* The autophagy-senescence connection in chemotherapy: must tumor cells (self) eat before they sleep? *J Pharmacol Exp Ther*. 2012;343:763-778.

68 Bandiera E, Todeschini P, Romani C *, et al.* The HIV-protease inhibitor saquinavir reduces proliferation, invasion and clonogenicity in cervical cancer cell lines. *Oncol Lett*. 2016;12:2493-2500.

69 Grune T, Merker K, Jung T *, et al.* Protein oxidation and degradation during postmitotic senescence. *Free Radic Biol Med*. 2005;39:1208-1215.

70 Davalli P, Mitic T, Caporali A *, et al.* ROS, Cell Senescence, and Novel Molecular Mechanisms in Aging and Age-Related Diseases. *Oxid Med Cell Longev*. 2016;2016:3565127.

71 Chandrasekaran A, Idelchik M, Melendez JA. Redox control of senescence and age-related disease. *Redox Biol*. 2017;11:91-102.

72 Jin L, Li C, Xu Y *, et al.* Epigallocatechin gallate promotes p53 accumulation and activity via the inhibition of MDM2-mediated p53 ubiquitination in human lung cancer cells. *Oncol Rep*. 2013;29:1983-1990.

73 Xue W, Zender L, Miething C *, et al.* Senescence and tumour clearance is triggered by p53 restoration in murine liver carcinomas. *Nature*. 2007;445:656-660.

74 Melnikova VO, Bolshakov SV, Walker C *, et al.* Genomic alterations in spontaneous and carcinogen-induced murine melanoma cell lines. *Oncogene*. 2004;23:2347-2356.

75 Chan CH, Gao Y, Moten A *, et al.* Novel ARF/p53-independent senescence pathways in cancer repression. *J Mol Med (Berl)*. 2011;89:857-867.

76 Nishio K, Inoue A. Senescence-associated alterations of cytoskeleton: extraordinary production of vimentin that anchors cytoplasmic p53 in senescent human fibroblasts. *Histochem Cell Biol*. 2005;123:263-273.

77 Chen QM, Tu VC, Catania J *, et al.* Involvement of Rb family proteins, focal adhesion proteins and protein synthesis in senescent morphogenesis induced by hydrogen peroxide. *J Cell Sci*. 2000;113 (Pt 22):4087-4097.

78 Goldmann WH, Auernheimer V, Thievessen I *, et al.* Vinculin, cell mechanics and tumour cell invasion. *Cell Biol Int*. 2013;37:397-405.

79 Dotto GP. Crosstalk of Notch with p53 and p63 in cancer growth control. *Nat Rev Cancer*. 2009;9:587-595.

80 Kwon C, Cheng P, King IN *, et al.* Notch post-translationally regulates beta-catenin protein in stem and progenitor cells. *Nat Cell Biol*. 2011;13:1244-1251.

81 Olmeda D, Castel S, Vilaro S *, et al.* Beta-catenin regulation during the cell cycle: implications in G2/M and apoptosis. *Mol Biol Cell*. 2003;14:2844-2860.

82 Kobayashi K, Takahashi H, Inoue A *, et al.* Oct-3/4 promotes migration and invasion of glioblastoma cells. *J Cell Biochem*. 2012;113:508-517.

83 Ip CK, Cheung AN, Ngan HY *, et al.* p70 S6 kinase in the control of actin cytoskeleton dynamics and directed migration of ovarian cancer cells. *Oncogene*. 2011;30:2420-2432.

84 Mok KW, Mruk DD, Silvestrini B *, et al.* rpS6 Regulates blood-testis barrier dynamics by affecting F-actin organization and protein recruitment. *Endocrinology*. 2012;153:5036-5048.

85 Yentrapalli R, Azimzadeh O, Sriharshan A *, et al.* The PI3K/Akt/mTOR pathway is implicated in the premature senescence of primary human endothelial cells exposed to chronic radiation. *PLoS One*. 2013;8:e70024.

86 Drewe J, Gutmann H, Fricker G *, et al.* HIV protease inhibitor ritonavir: a more potent inhibitor of P-glycoprotein than the cyclosporine analog SDZ PSC 833. *Biochem Pharmacol*. 1999;57:1147-1152.

87 Donia M, Mangano K, Fagone P *, et al.* Unique antineoplastic profile of Saquinavir-NO, a novel NO-derivative of the protease inhibitor Saquinavir, on the in vitro and in vivo tumor formation of A375 human melanoma cells. *Oncol Rep*. 2012;28:682-688.

88 Donia M, Maksimovic-Ivanic D, Mijatovic S *, et al.* In vitro and in vivo anticancer action of Saquinavir-NO, a novel nitric oxide-derivative of the protease inhibitor saquinavir, on hormone resistant prostate cancer cells. *Cell Cycle*. 2011;10:492-499.

89 Paskas S, Mazzon E, Basile MS *, et al.* Lopinavir-NO, a nitric oxide-releasing HIV protease inhibitor, suppresses the growth of melanoma cells in vitro and in vivo. *Invest New Drugs*. 2019;

Figure legends:

Table 1: IC_{50} values of Ritonavir and NO-modified Ritonavir. Data are presented as mean± SEM of three independent experiments.

Figure 1: Tested HIV-PIs induce inhibition of proliferation, with minor apoptosis in both cell lines. B16 and B16F10 cells were treated with IC_{50} values of tested compounds for 48 h,

and then subjected to: (A) CFSE, (B) Annexin/propidium iodide and (C) Apostat staining. Cells were analyzed by flow cytometry. One representative experiment out of three is shown. (D) cells were stained with propidium iodide and observed under a fluorescent microscope, 250X magnification.

Figure 2: Treatment with Ritonavir and its derivative does not induce differentiation towards melanocytes nor Schwann-like cells. (A) Melanin production and tyrosinase activity were measured as markers of melanocyte differentiation. Data are presented as mean± SEM of three independent experiments. (B) Immunocytochemical staining of myelin basic protein. One representative staining out of three is shown, magnification 1000X.

Figure 3: Ritonavir and Ritonavir-NO promote melanoma senescence and persistent proliferation inhibition. (A) β-galactosidase activity was measured in samples treated with IC_{50} doses of HIV-PIs. One representative experiment out of three is shown. (B) Melanoma cells were treated with Ritonavir and Ritonavir-NO for 48 h and the presence of lipofuscin granules was evaluated by histochemistry (magnification 1000X). (C)Melanoma cells were treated with Ritonavir and Ritonavir-NO for 48 h. After treatment, cells were seeded in a concentration 2000 cells/ well in a medium without HIV-PIs and colony formation was followed for five consecutive days. The data are presented as the percentage of control ± SEM from three independent experiments. *p<0.05, **p<0.01, ***p<0.001 refers to untreated cultures, calculated by ANOVA.

Figure 4: Tested compounds provoke ROS/RNS production, but not an intracellular NO release. After treatment with IC_{50} doses of Ritonavir and Ritonavir-NO for 48 h, cells were subjected to (A) DAF-FM staining or (B) DHR staining and analyzed by flow cytometry. One representative experiment out of three is shown.

Figure 5: Progenitor signaling pathways in responce to HIV-PIs. B16 and B16F10 melanoma were treated with HIV-PIs for the indicated time points. The expression was

analyzed by western blot. Densitometric analysis of data is presented as fold change obtained by normalization to GAPDH and then normalization to control. One representative experiment out of three is shown.

Figure 6: Downstream members of mTOR signaling pathway in responce to HIV-PIs. B16 and B16F10 melanoma were treated with Ritonavir and Ritonavir-NO for the indicated time points. The expression was analyzed by western blot. Densitometric analysis of data is presented as fold change obtained by normalization to an unphosphorylated proteins and then normalization to control. One representative experiment out of three is shown.

Supplement 1: Ritonavir and Ritonavir-NO reduced the viability of melanoma cell lines in a dose-dependent manner. Mouse primary melanoma (B16), mouse metastatic melanoma (B16F10) and human melanoma (A375) cell lines were treated with Ritonavir and Ritonavir-NO in doses from 0 to 80 μM for 48 h. Cell viability was determined by MTT and CV assay. The data are presented as percentage of control ± SD from one representative experiment out of three. *$p<0.05$ refers to untreated cultures.

Supplement 2: Ritonavir and Ritonavir-NO induce a morphological change of melanoma cell lines. Mouse primary melanoma (B16) and metastatic melanoma (B16F10) cell lines were treated with IC_{50} concentrations of Ritonavir and Ritonavir-NO for 48 h and observed under a light microscope Nikon TS 100 (Nikon, Tokyo, Japan), 100X magnification.

Supplement 3: Ritonavir and Ritonavir-NO increase cell granularity. Mouse primary melanoma (B16) and metastatic melanoma cell line (B16F10) were treated with IC_{50} concentrations of Ritonavir and Ritonavir-NO for 48 h and analysed by flow cytometry. One representative experiment out of three is shown.

Supplement 4: Cytoskeletal proteins and p53 in responce to HIV-PIs. B16 and B16F10 melanoma were treated with 16 µM Ritonavir and 8 µM Ritonavir-NO for the indicated time points. The expression was analyzed by western blot. Densitometric analysis of data is presented as fold change obtained by normalization to GAPDH and then normalization to control. One representative experiment out of three is shown.

Supplement 5: Ritonavir and Ritonavir-NO induce oxidative stress which does not reduce the viability of melanoma cells. B16 and B16F10 cell lines were treated with IC_{50} concentrations of Ritonavir and Ritonavir-NO (HIV-PI) in combination with antioxidant N-acetylcysteine (N-ac, 2.5 µM) for 48 h and stained with crystal violet. The data are presented as a percentage of control± SEM from three independent experiments. Bars not sharing a common letter are significantly different, $p<0.05$, calculated using Kruskal Wallis test.

Figure 1

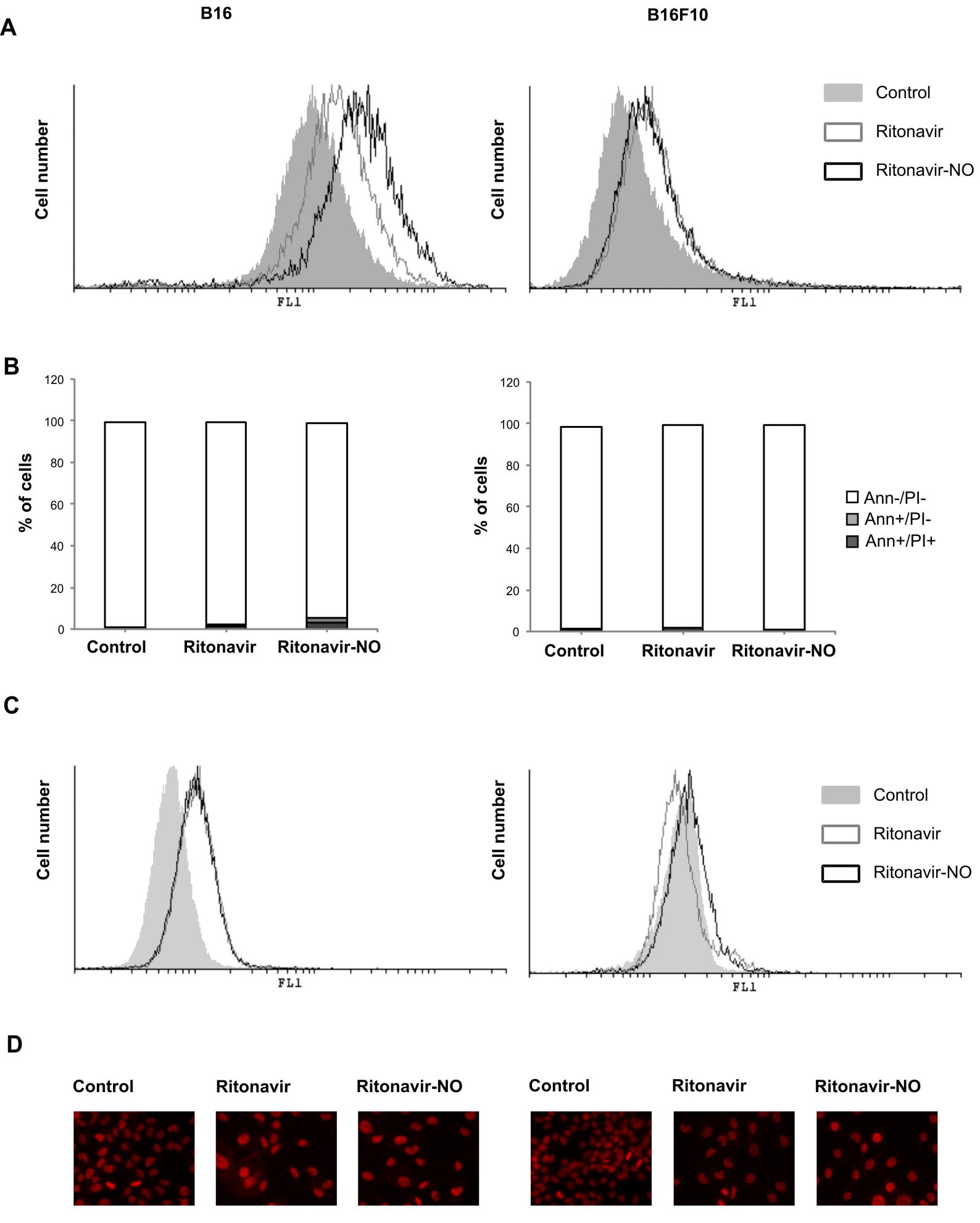
A
B16
B16F10
Cell number
FL1
Control
Ritonavir
Ritonavir-NO
B
% of cells
120
100
80
60
40
20
0
Control
Ritonavir
Ritonavir-NO
Ann-/PI-
Ann+/PI-
Ann+/PI+
C
Cell number
FL1
Control
Ritonavir
Ritonavir-NO
D
Control
Ritonavir
Ritonavir-NO
Control
Ritonavir
Ritonavir-NO

Figure 2

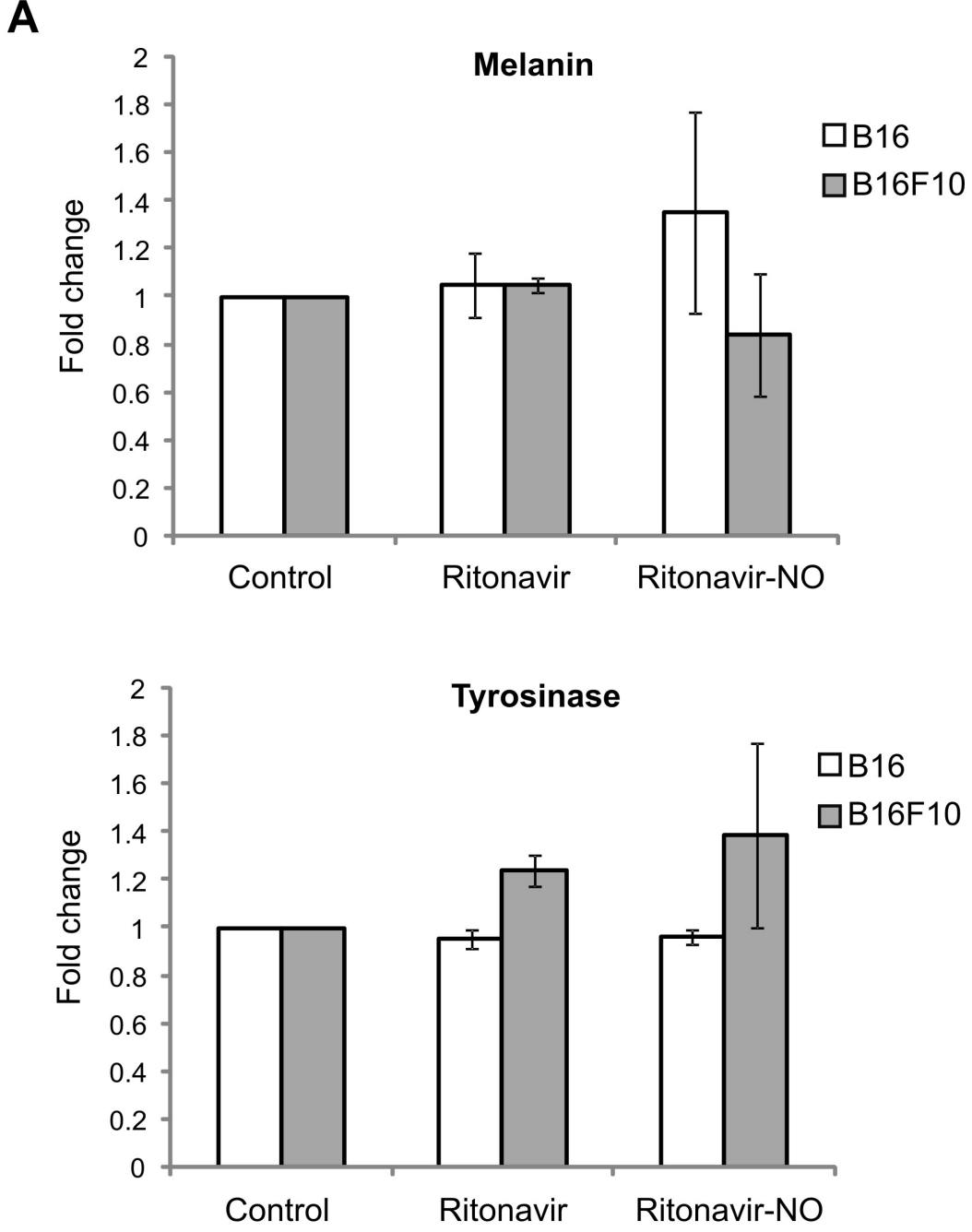
A
Melanin
Fold change
2
1.8
1.6
1.4
1.2
1
0.8
0.6
0.4
0.2
0
B16
B16F10
Control
Ritonavir
Ritonavir-NO
Tyrosinase
Fold change
2
1.8
1.6
1.4
1.2
1
0.8
0.6
0.4
0.2
0
B16
B16F10
Control
Ritonavir
Ritonavir-NO

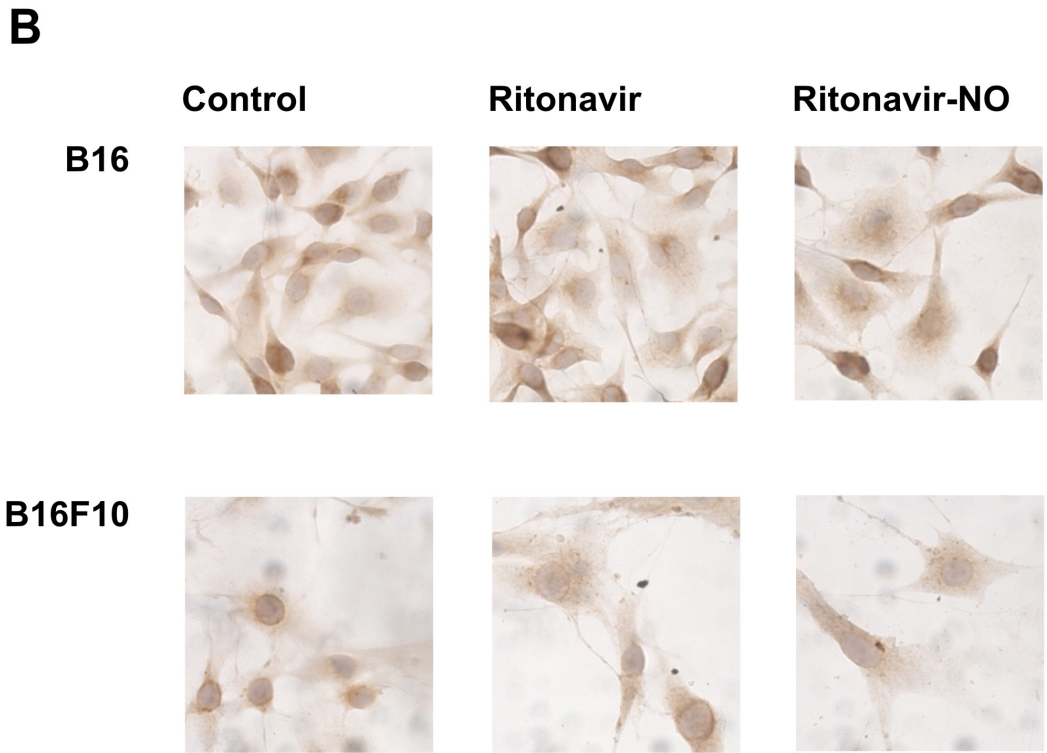
B
Control
Ritonavir
Ritonavir-NO
B16
B16F10

Figure 3

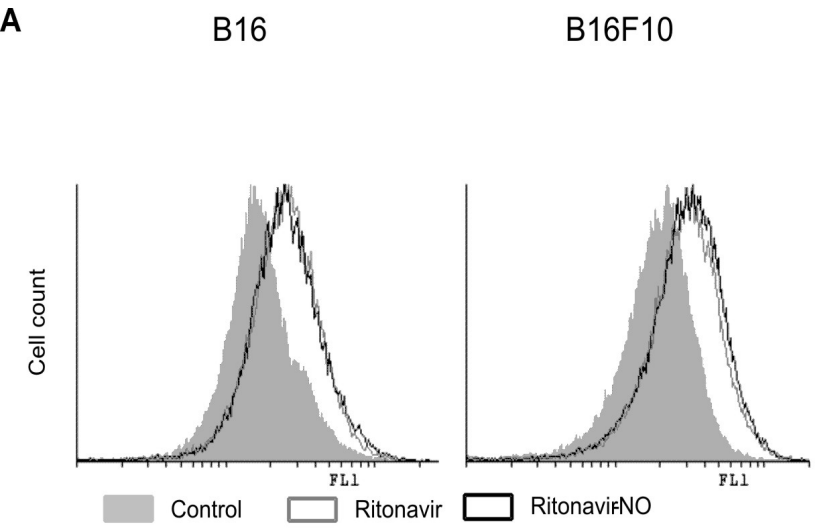
A
B16
B16F10
Cell count
FL1
FL1
Control
Ritonavir
Ritonavir-NO

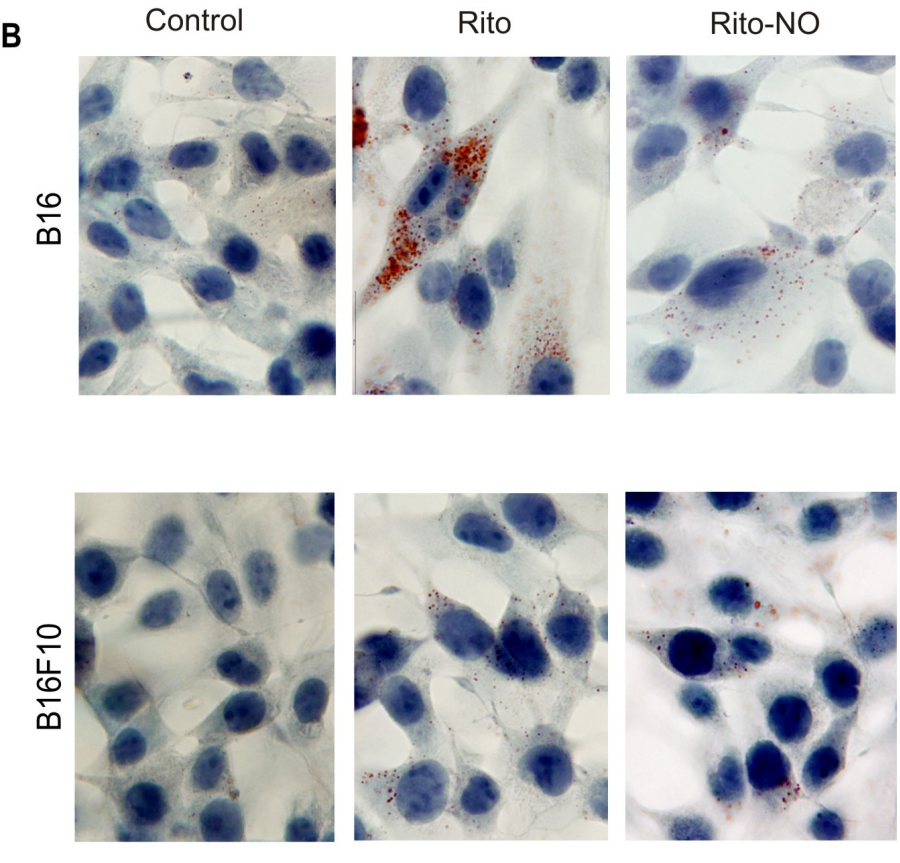
B
Control
Rito
Rito-NO
B16
B16F10

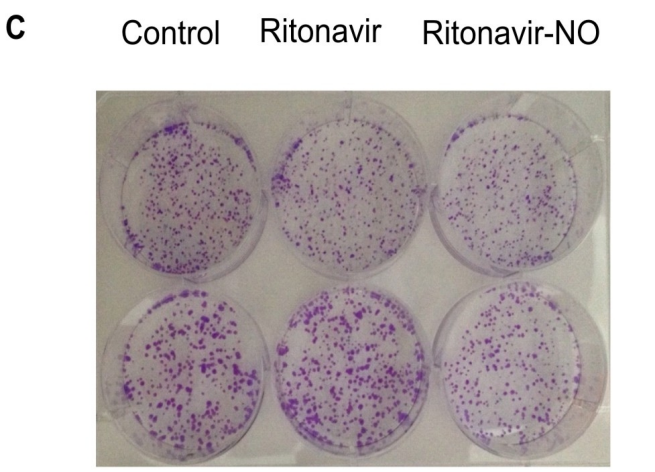
C
Control
Ritonavir
Ritonavir-NO

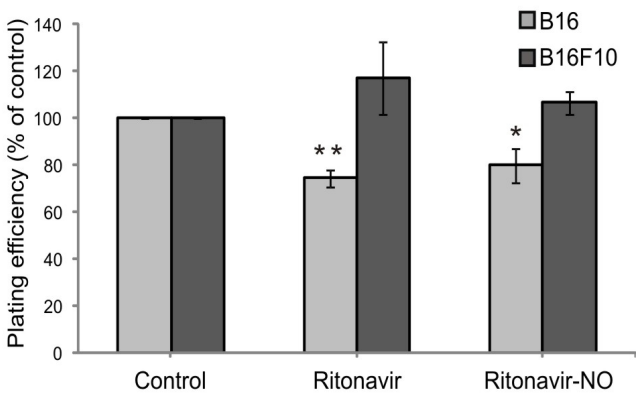
Plating efficiency (% of control)
B16
B16F10
Control
Ritonavir
Ritonavir-NO

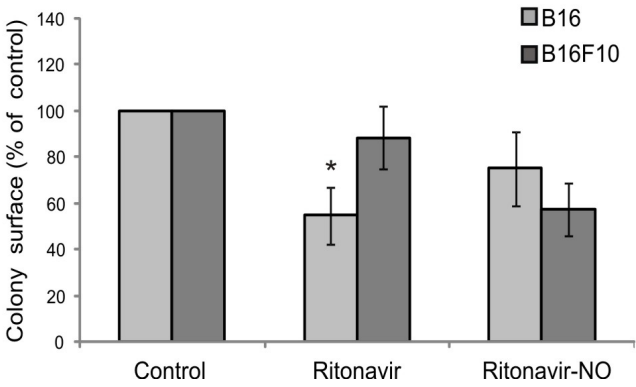
Colony surface (% of control)
B16
B16F10
Control
Ritonavir
Ritonavir-NO

Figure 4

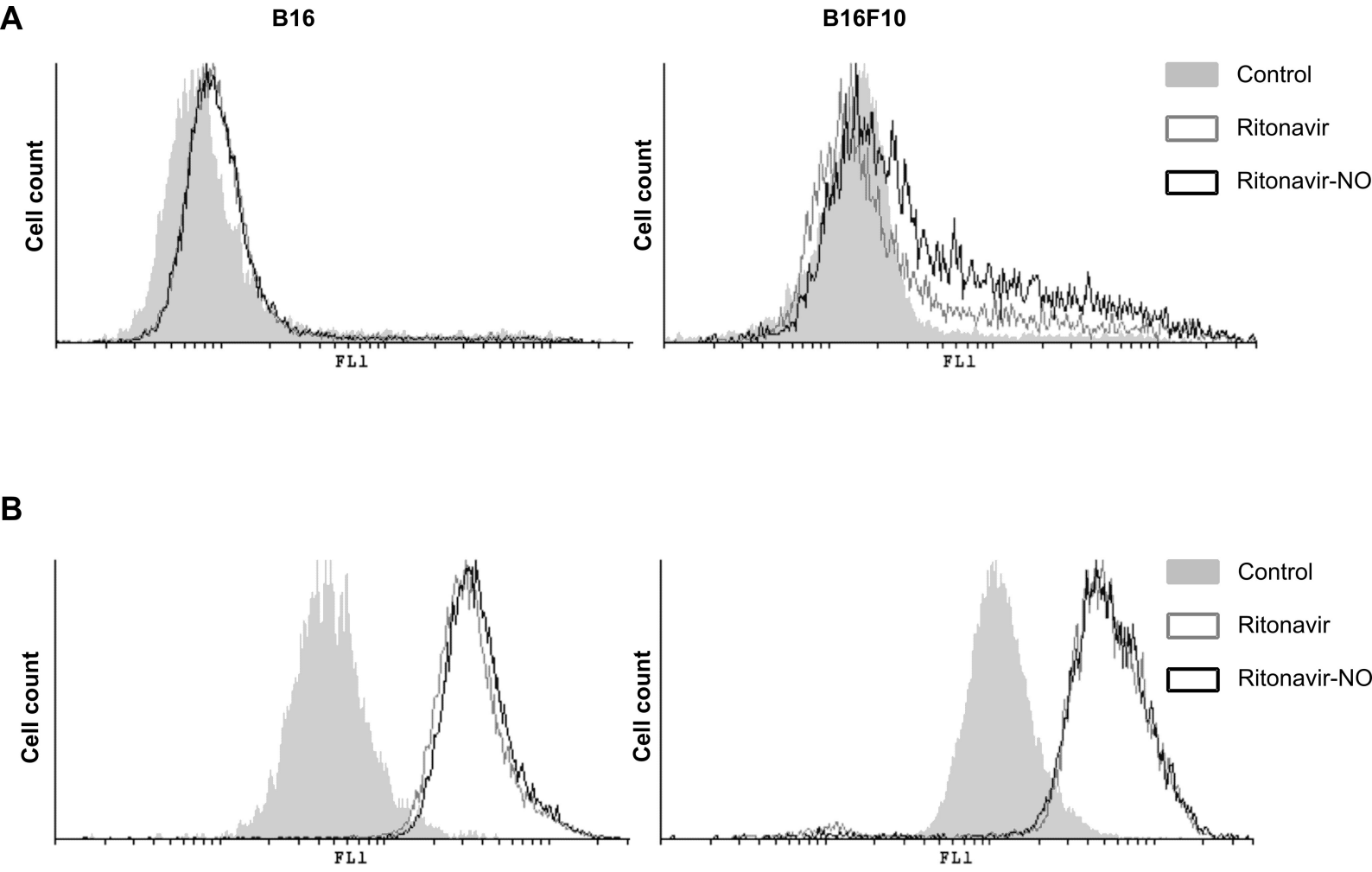
A
B16
B16F10
Cell count
FL1
Control
Ritonavir
Ritonavir-NO

B
Cell count
FL1
Control
Ritonavir
Ritonavir-NO

Figure 5

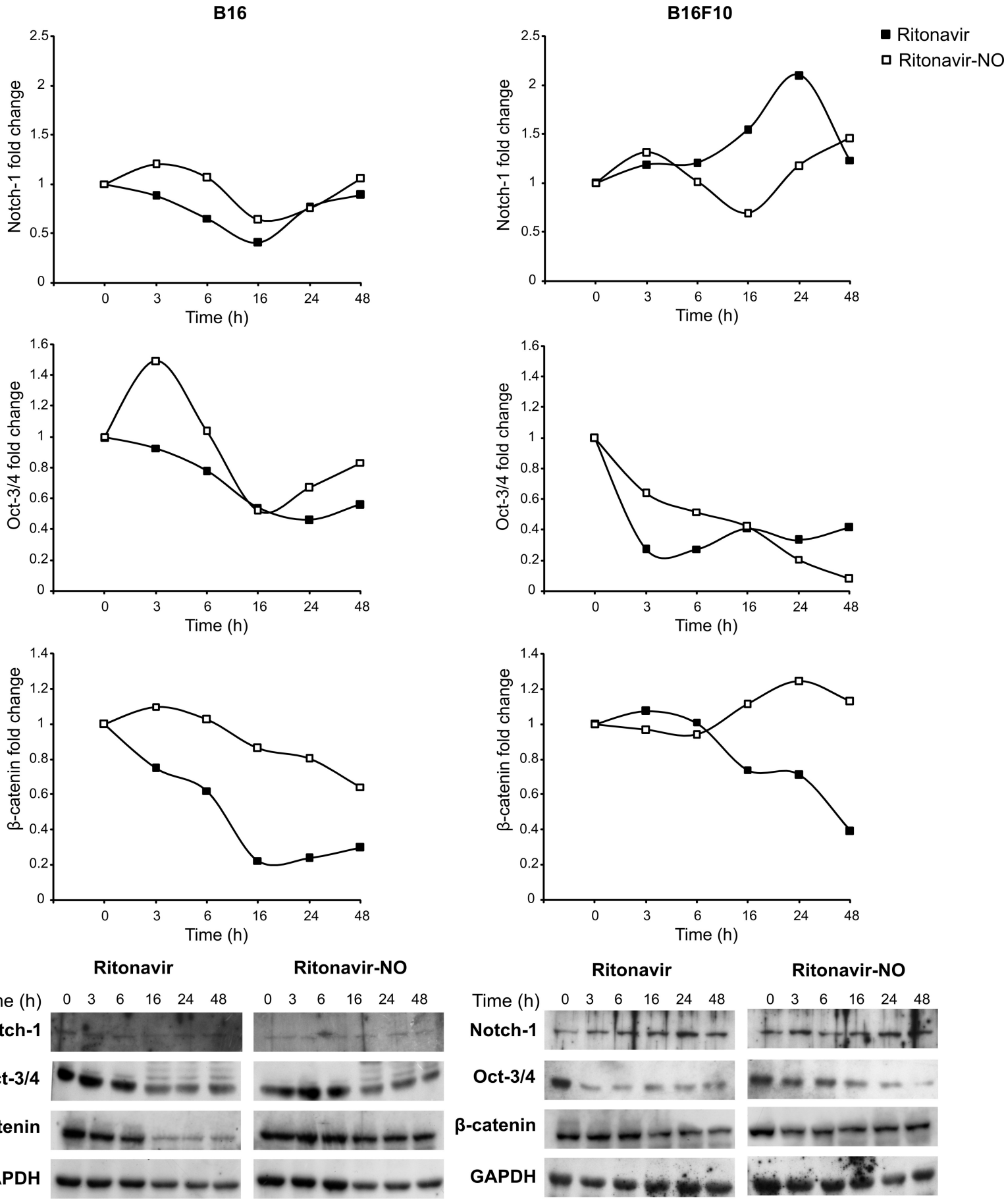
B16
B16F10
Ritonavir
Ritonavir-NO
Notch-1 fold change
Oct-3/4 fold change
β-catenin fold change
Time (h)
0 3 6 16 24 48
Ritonavir
Ritonavir-NO
Time (h)
Notch-1
Oct-3/4
β-catenin
GAPDH

Figure 6

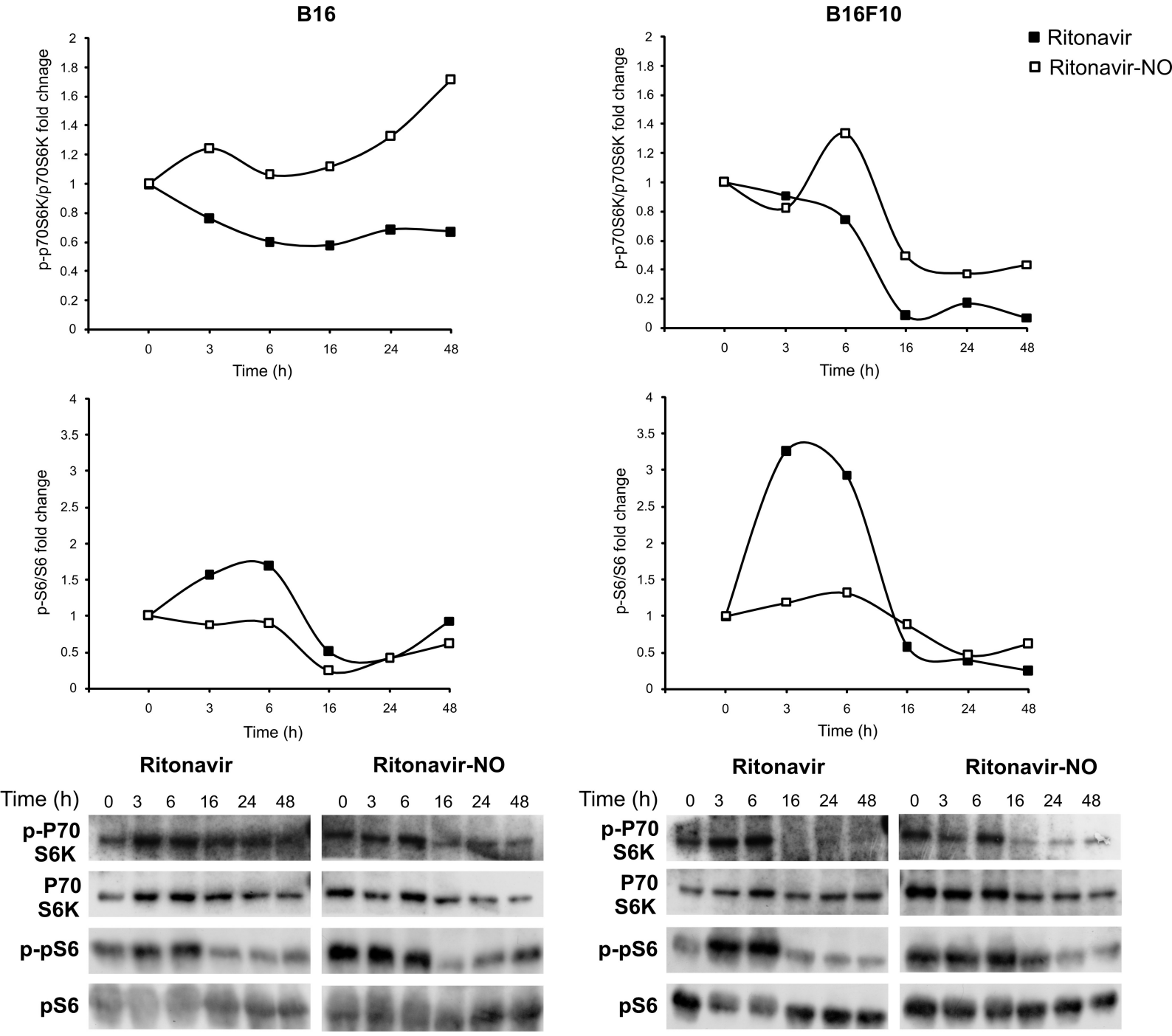
B16
B16F10
Ritonavir
Ritonavir-NO
p-p70S6K/p70S6K fold chnage
p-p70S6K/p70S6K fold change
Time (h)
p-S6/S6 fold change
Ritonavir
Ritonavir-NO
Time (h)
p-P70 S6K
P70 S6K
p-pS6
pS6

Suppl 1

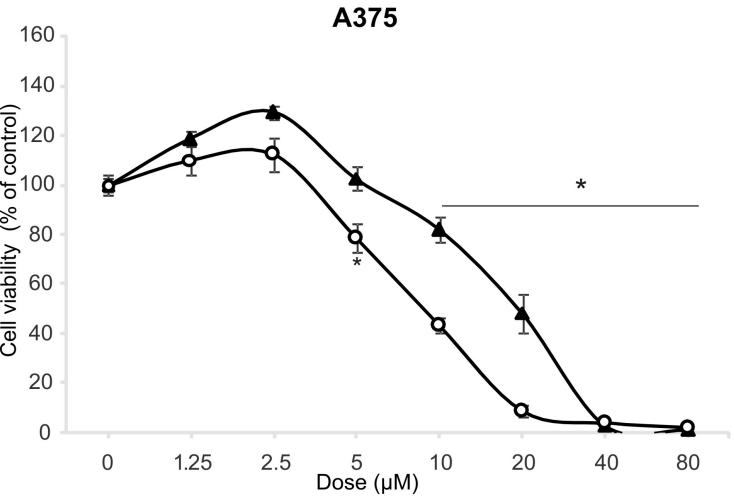
A375
Cell viability (% of control)
160
140
120
100
80
60
40
20
0
0
1.25
2.5
5
10
20
40
80
Dose (μM)
*
*

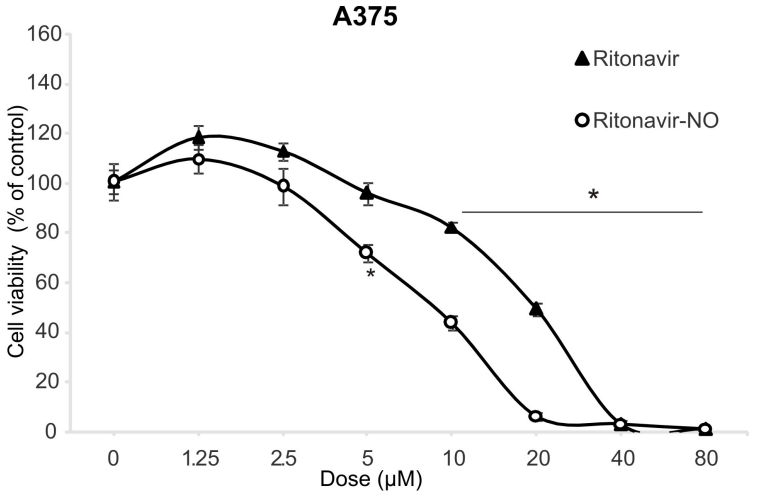
A375
Ritonavir
Ritonavir-NO
Cell viability (% of control)
160
140
120
100
80
60
40
20
0
0
1.25
2.5
5
10
20
40
80
Dose (μM)
*
*

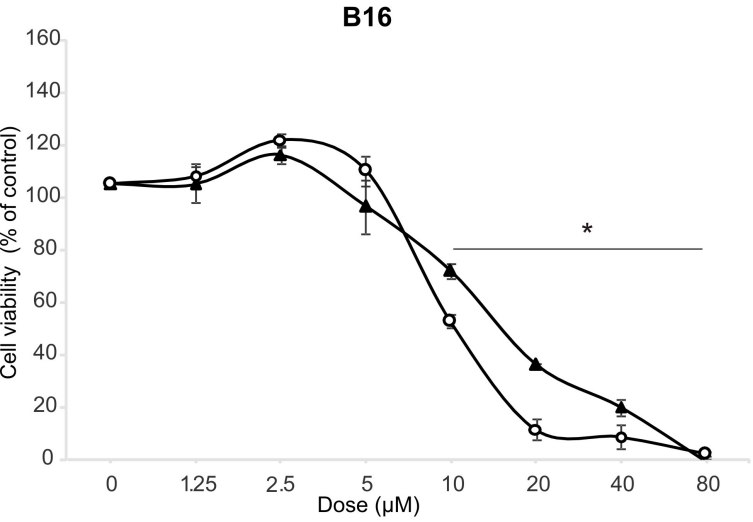
B16
Cell viability (% of control)
160
140
120
100
80
60
40
20
0
0
1.25
2.5
5
10
20
40
80
Dose (μM)
*

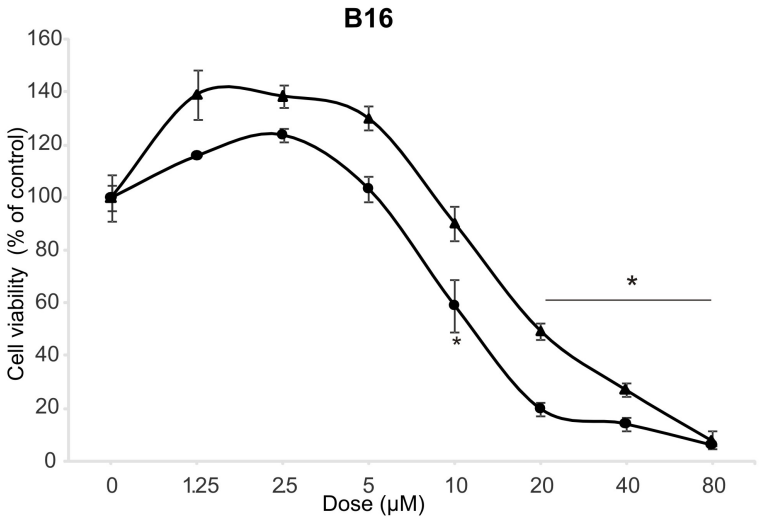
B16
Cell viability (% of control)
160
140
120
100
80
60
40
20
0
0
1.25
2.5
5
10
20
40
80
Dose (μM)
*
*

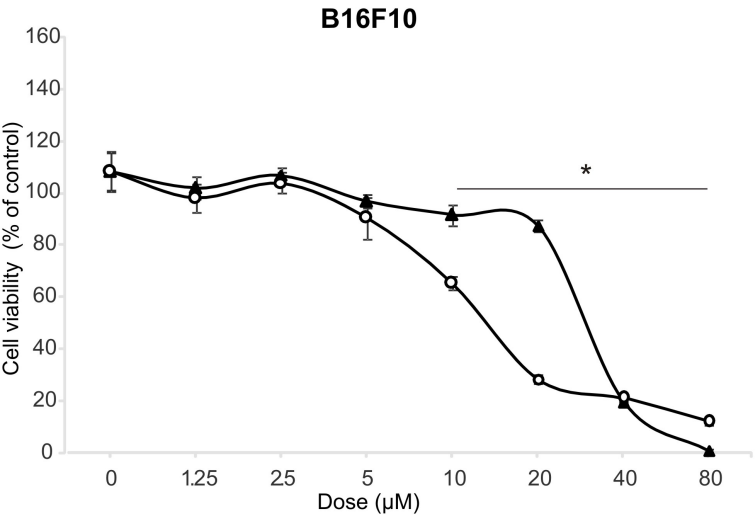
B16F10
Cell viability (% of control)
160
140
120
100
80
60
40
20
0
0
1.25
2.5
5
10
20
40
80
Dose (μM)
*

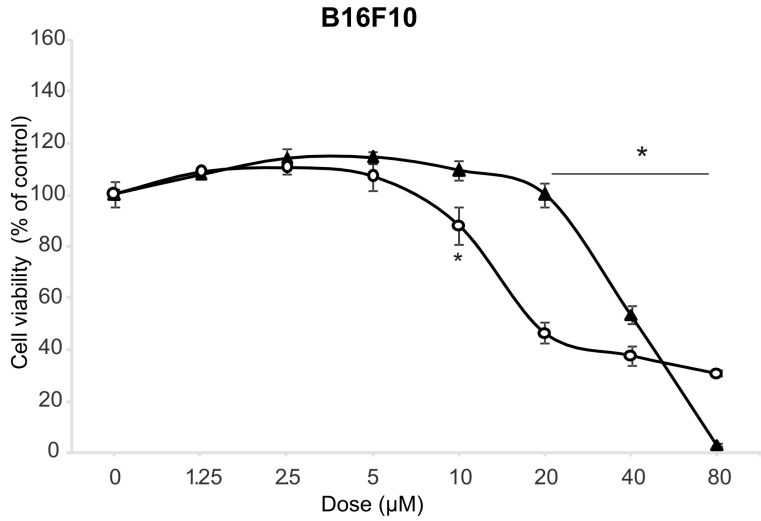
B16F10
Cell viability (% of control)
160
140
120
100
80
60
40
20
0
0
1.25
2.5
5
10
20
40
80
Dose (μM)
*
*

Suppl 2

B16

Control

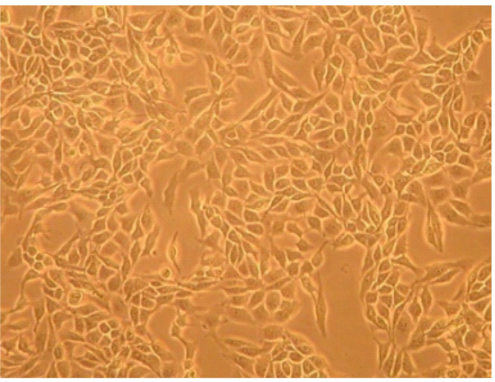

Ritonavir

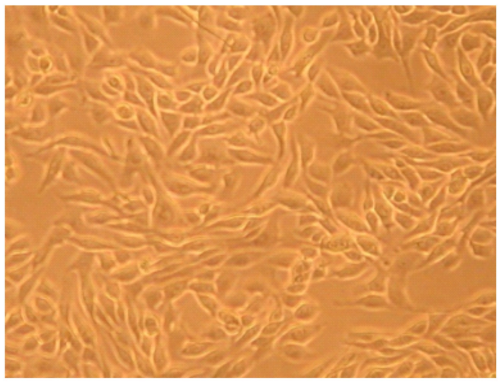

Ritonavir-NO

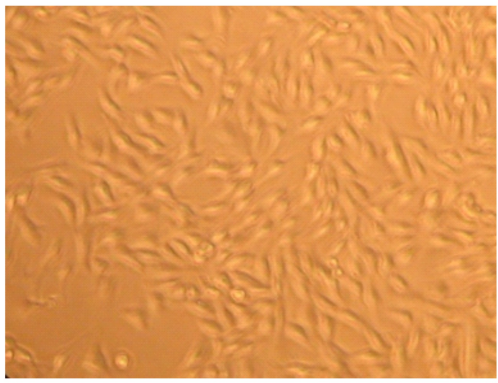

B16F10

Control

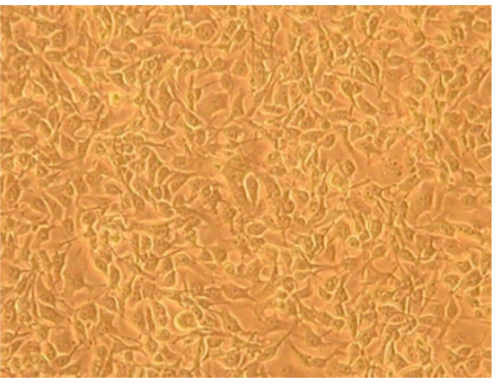

Ritonavir

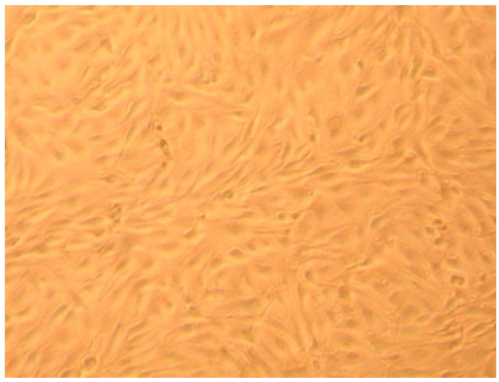

Ritonavir-NO

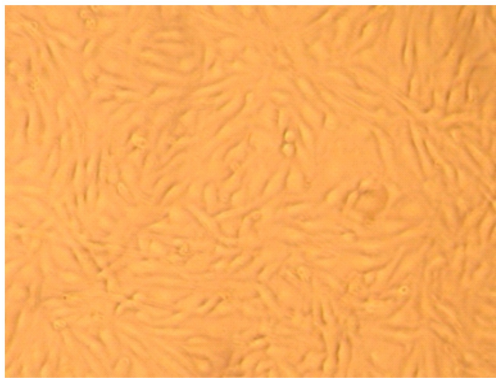

Suppl 3

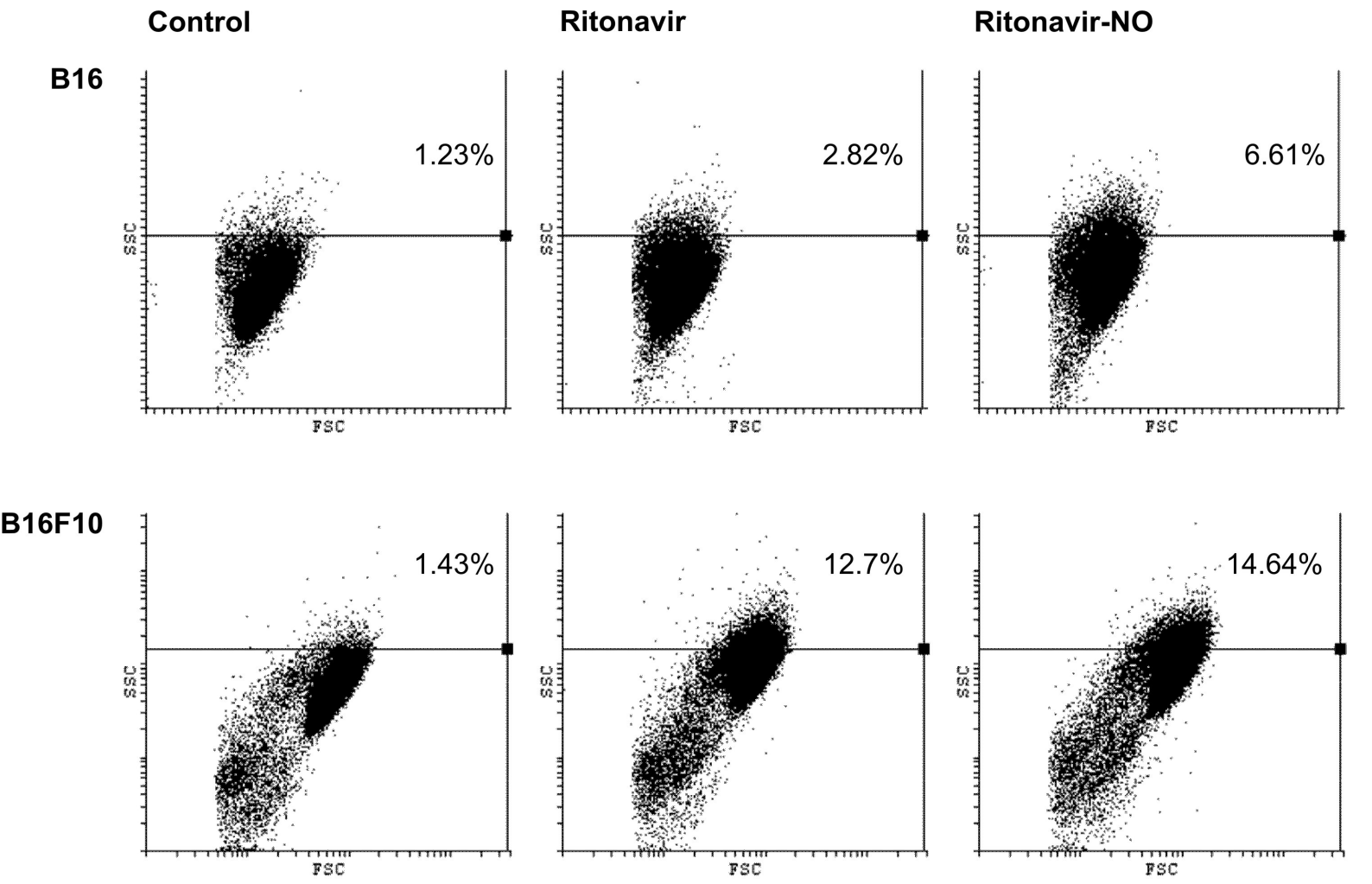
Control
Ritonavir
Ritonavir-NO
B16
1.23%
2.82%
6.61%
B16F10
1.43%
12.7%
14.64%
SSC
FSC

Suppl 4

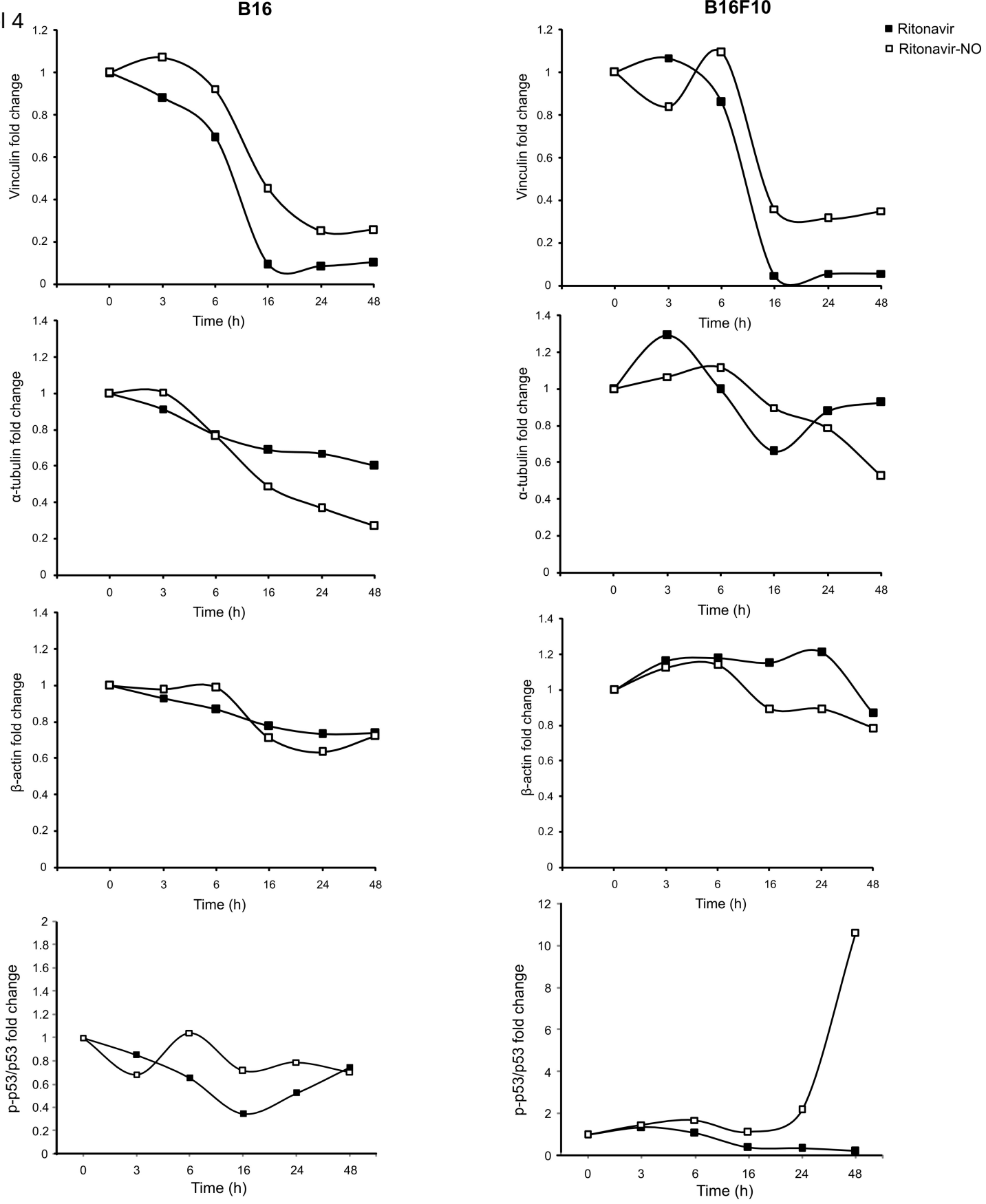
B16
B16F10
Ritonavir
Ritonavir-NO
Vinculin fold change
α-tubulin fold change
β-actin fold change
p-p53/p53 fold change
Time (h)
0 3 6 16 24 48

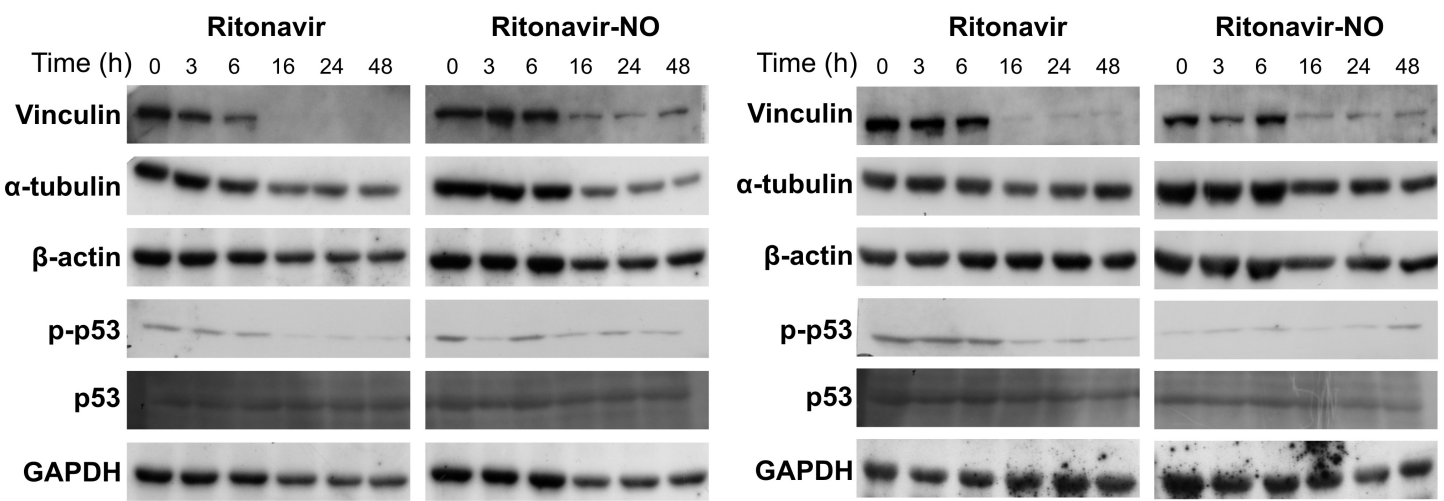
Ritonavir
Ritonavir-NO
Time (h) 0 3 6 16 24 48
Vinculin
α-tubulin
β-actin
p-p53
p53
GAPDH

Suppl 5

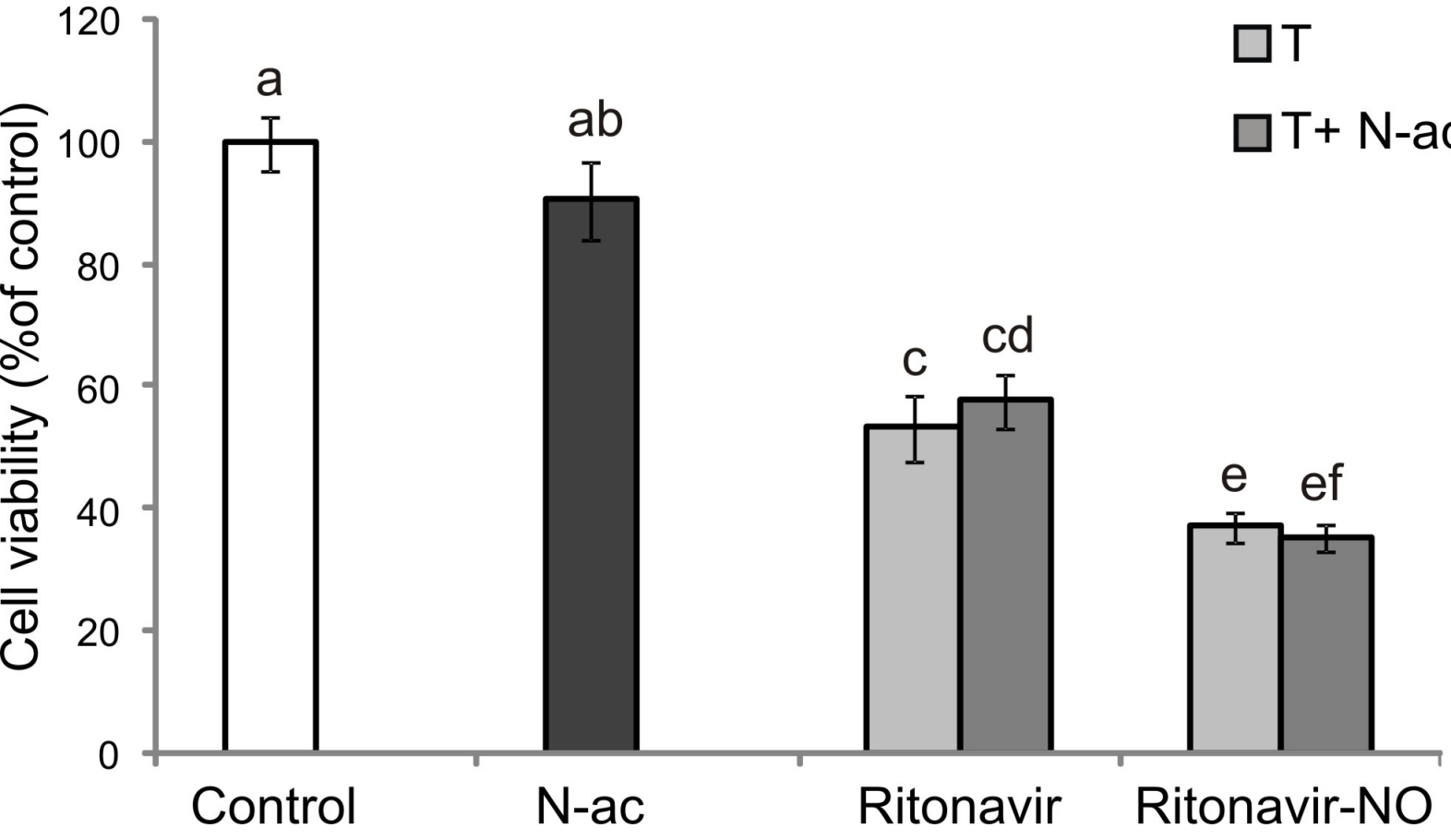
120
100
80
60
40
20
0
Cell viability (%of control)
a
ab
c
cd
e
ef
T
T+ N-ac
Control
N-ac
Ritonavir
Ritonavir-NO

Table 1

IC_{50} values of Ritonavir and Ritonavir-NO in melanoma cell lines

Cell line	Assay	IC_{50} (μM)	
		Ritonavir	Ritonavir-NO
A375	MTT	14.99 ± 1.95	6.33 ± 1.11
	CV	14.84 ± 2.22	6.59 ± 0.59
B16	MTT	15.32 ± 2	8.15 ± 0.19
	CV	15.88 ± 1.31	9.2 ± 0.85
B16F10	MTT	24.62 ± 1.18	9.65 ± 1.04
	CV	30.66 ± 3.47	14.94 ± 0.59